

This is the accepted manuscript made available via CHORUS. The article has been published as:

## Effect of Van Hove singularities on high- $T_c$ superconductivity in $H_3S$

Wataru Sano, Takashi Koretsune, Terumasa Tadano, Ryosuke Akashi, and Ryotaro Arita

Phys. Rev. B **93**, 094525 — Published 31 March 2016

DOI: [10.1103/PhysRevB.93.094525](https://doi.org/10.1103/PhysRevB.93.094525)

# Effect of van Hove singularities on high- $T_c$ superconductivity in $\text{H}_3\text{S}$

Wataru Sano,<sup>1,2</sup> Takashi Koretsune,<sup>2,3,\*</sup> Terumasa Tadano,<sup>1</sup> Ryosuke Akashi,<sup>4</sup> and Ryotaro Arita<sup>2,5</sup>

<sup>1</sup>*Department of Applied Physics, University of Tokyo,  
7-3-1 Hongo, Bunkyo-ku, Tokyo 113-8656, Japan*

<sup>2</sup>*RIKEN Center for Emergent Matter Science, 2-1 Hirosawa, Wako, Saitama 351-0198, Japan*

<sup>3</sup>*JST, PRESTO, 4-1-8 Honcho, Kawaguchi, Saitama 332-0012, Japan*

<sup>4</sup>*Department of Physics, University of Tokyo, 7-3-1 Hongo, Bunkyo-ku, Tokyo 113-0033, Japan*

<sup>5</sup>*ERATO Isobe Degenerate -Integration Project, Tohoku University, Aoba-ku, Sendai 980-8578, Japan*

(Dated: March 11, 2016)

One of interesting open questions for the high transition temperature ( $T_c$ ) superconductivity in sulfur hydrides is why high pressure phases of  $\text{H}_3\text{S}$  have extremely high  $T_c$ 's. Recently, it has been pointed out that the presence of the van Hove singularities (vHs) around the Fermi level is crucial. However, while there have been quantitative estimates of  $T_c$  based on the Migdal-Eliashberg theory, the energy dependence of the density of states (DOS) has been neglected to simplify the Eliashberg equation. In this study, we go beyond the constant DOS approximation and explicitly consider the electronic structure over 40 eV around the Fermi level. In contrast with the previous conventional calculations, this approach with a sufficiently large number of Matsubara frequencies enables us to calculate  $T_c$  without introducing the empirical pseudo Coulomb potential. We show that while  $\text{H}_3\text{S}$  has much higher  $T_c$  than  $\text{H}_2\text{S}$  for which the vHs is absent, the constant DOS approximation employed so far seriously overestimates (underestimates)  $T_c$  by  $\sim 60$  K ( $\sim 10$  K) for  $\text{H}_3\text{S}$  ( $\text{H}_2\text{S}$ ). We then discuss the impact of the strong electron-phonon coupling on the electronic structure with and without the vHs and how it affects the superconductivity. Especially, we focus on (1) the feedback effect in the self-consistent calculation of the self-energy, (2) the effect of the energy shift due to the zero-point motion, and (3) the effect of the changes in the phonon frequencies due to strong anharmonicity. We show that the effect of (1)-(3) on  $T_c$  is about 10-30 K for both  $\text{H}_3\text{S}$  and  $\text{H}_2\text{S}$ . Eventually,  $T_c$  is estimated to be 181 K for  $\text{H}_3\text{S}$  at 250 GPa and 34 K for  $\text{H}_2\text{S}$  at 140 GPa, which explains the pressure dependence of  $T_c$  observed in the experiment. In addition, we evaluate the lowest order vertex correction beyond the Migdal-Eliashberg theory and discuss the validity of the Migdal approximation for sulfur hydrides.

PACS numbers: 74.62.Fj, 63.20.dk, 71.15.Mb, 74.25.Jb

## I. INTRODUCTION

Realization of superconductivity at very high temperatures has been the Holy Grail in condensed matter physics. While unconventional superconductors such as the cuprates [1] and iron-based superconductors [2] have been extensively studied, the mechanism for the high transition temperatures ( $T_c$ 's) is yet to be fully understood. On the other hand, there has been a simple but promising strategy to achieve high  $T_c$  for conventional phonon mediated superconductors [3–5]. According to the BCS theory [6],  $T_c$  is scaled by the inverse square root of the atomic mass. Thus, compounds comprising light elements are promising candidates for high- $T_c$  superconductors. Indeed, high- $T_c$  superconductivity has been found so far in a variety of light-element compounds such as the graphite intercalation compounds [7], elemental lithium under high pressures [8–10], magnesium diboride [11], and boron-doped diamond [12, 13].

Since hydrogen has the lightest atomic mass, the metallic hydrogen [3, 4] or hydrogen-rich compounds [5] have been long expected to be high- $T_c$  superconductors.

Recently, it has been reported that  $\text{H}_2\text{S}$  under pressures of 100-200 GPa exhibits superconductivity at extremely high temperatures up to  $\sim 200$  K [14, 15], breaking the record of the cuprates [16, 17].

Prior and after this experimental discovery, there are a lot of *ab initio* studies for compressed sulfur hydrides [18–37]. A variety of possible crystal structures have been found by structure searching calculations [18, 19, 23, 36, 37], and  $T_c$  has been estimated to be lower than 100 K (as high as 200 K) for  $\text{H}_2\text{S}$  ( $\text{H}_3\text{S}$ ) [19, 22, 25–27, 29, 34, 36]. It is also suggested that chemical substitution of sulfur atoms could enhance  $T_c$  [31, 32]. Most of these works have concluded that the compressed sulfur hydrides are phonon-mediated strong-coupling superconductors. Not only the existence of high frequency phonons due to the hydrogen motion, strong electron-phonon coupling has also been shown to be important for high- $T_c$  superconductivity, especially in  $\text{H}_3\text{S}$ . These results are indeed consistent with the experiment [14, 15, 38] where the isotope effect is observed to be significant.

Interestingly, in the calculations based on the Migdal-Eliashberg (ME) theory [39, 40], there is a clear difference in calculated  $T_c$ 's between  $\text{H}_2\text{S}$  and  $\text{H}_3\text{S}$ . While the origin of this difference is yet to be fully understood, recently, it has been suggested that van Hove singularities (vHs) in the electronic structure of  $\text{H}_3\text{S}$  play a key role to under-

---

\*Electronic address: takashi.koretsune@riken.jp

stand this problem [24, 28, 30, 33]. It is noteworthy that this situation is similar to that of the A15 compounds, for which the density of states (DOS) has a sharp peak around the Fermi level [41–45]. Indeed, there have been some model calculations which studied how the energy dependence of the DOS affects  $T_c$  [42]. On the other hand, for  $\text{H}_3\text{S}$ , the effect of the vHs on the superconductivity has not been fully understood. In the previous studies based on the ME theory [18–20, 34], the DOS is assumed to have no energy dependence. This is mainly because one can reduce the numerical cost to solve the Eliashberg equation.

In this study, we examine how the presence/absence of the vHs affects  $T_c$  of sulfur hydrides. To this end, we go beyond the constant DOS approximation. With a sufficiently large number of Matsubara frequencies, the retardation effect is automatically considered. Such a calculation is possible because the ratio between  $T_c$  and the band width is only  $\mathcal{O}(10^{-3})$ . Note that the ratio for usual conventional superconductors is as small as  $\mathcal{O}(10^{-5})$  so that the retardation effect is represented by introducing the empirical pseudo Coulomb potential  $\mu^*$ .

Another advantage of the present approach is that we can calculate the self-energy due to the electron-phonon coupling self-consistently. As will be discussed in Sec. II, in the constant DOS approximation, the feedback effect included in self-consistent calculation is automatically neglected. Also in the standard density functional theory for superconductors [25, 26, 46], the exchange correlation functional representing the mass enhancement effect is not calculated self-consistently. In this study, we discuss how the self-consistency in the calculation of the self-energy affects the superconductivity in the sulfur hydride superconductors.

In the calculation of the self-energy, we first consider the standard contribution (the lowest phonon-exchange diagram) in the ME theory. On top of that, we then study the effect of the so-called zero-point renormalization (ZPR), i.e., the band energy shift due to the zero-point motion. It should be noted that the amplitude of the zero-point motion of hydrogen atoms in sulfur hydrides is larger than 0.1 Å. Indeed, it has been proposed that its effect on the electronic structure and superconductivity is expected to be significant [28] and contribute to the stability of high-symmetry cubic phase [36].

Another characteristic feature of the superconducting sulfur hydrides is its strong anharmonic effect. Recently, within the constant DOS approximation, it has been shown that the anharmonicity in  $\text{H}_3\text{S}$  significantly suppresses the superconductivity, especially when the system experiences the second order structural phase transition (from  $R\bar{3}m$  to  $Im\bar{3}m$ ) [27]. In this work, we also study the anharmonic effect in the energy-dependent Eliashberg approach for  $\text{H}_3\text{S}$  and  $\text{H}_2\text{S}$ , and show that the impact of anharmonicity is significant not only in  $\text{H}_3\text{S}$  but also  $\text{H}_2\text{S}$ .

Finally, we study the validity of the ME theory. It has been suggested that the Migdal theorem [39] might

not be applicable to  $\text{H}_3\text{S}$  [28, 35], though  $T_c$  estimated by the ME theory is consistent with experimentally observed values. Since the effective Fermi energy at the vHs is small and comparable to the phonon energy scale, the premise of the ME theory might not be satisfied. Indeed, there has been a study proposing unconventional pairing mechanism [21]. Here we estimate the lowest order vertex correction beyond the ME theory and examine its effect on  $T_c$  [47].

This paper is organized as follows. In Sec. II we review the methods to study the normal and superconducting properties of solids from first-principles. In particular, we describe the approximations employed thus far to solve the linearized Eliashberg equation and discuss how we go beyond. Here we also describe how to treat the ZPR and anharmonicity. In Sec. III, we discuss the normal electronic structure and the phonon structure for  $\text{H}_3\text{S}$  with the  $Im\bar{3}m$  structure and  $\text{H}_2\text{S}$  with the  $P\bar{1}$  structure. In Sec. IV, we show that the constant DOS approximation seriously overestimates  $T_c$  of  $\text{H}_3\text{S}$  by  $\sim 60$  K. On the other hand, in the case of  $\text{H}_2\text{S}$  for which the vHs are absent, the constant DOS approximation underestimates  $T_c$  by  $\sim 10$  K. We then discuss how the self-energy due to the strong electron-phonon coupling affects the van Hove singularities and  $T_c$ . We study (1) the feedback effect in the self-consistent calculation of the self-energy, (2) the effect of the electron energy shift due to the zero-point motion, and (3) the effect of the changes in the phonon frequencies due to the strong anharmonicity. We show that the effect of (1)-(3) on  $T_c$  is about 10-30 K for both  $\text{H}_3\text{S}$  and  $\text{H}_2\text{S}$ , and  $T_c$  is estimated to be 181 K for  $\text{H}_3\text{S}$ , and 34 K for  $\text{H}_2\text{S}$ . These results suggest that  $\text{H}_3\text{S}$  ( $\text{H}_2\text{S}$ ) is responsible for the high- (low-)  $T_c$  superconductivity under pressures higher (lower) than  $\sim 150$  GPa. In Sec. VI, we evaluate the lowest order vertex correction and its effect on  $T_c$  in order to obtain the criterion for the justification of the ME theory. Finally, we give a summary of this study in Sec. VII.

## II. METHOD

### A. Migdal-Eliashberg theory for $T_c$ calculation with energy dependent DOS

Based on density functional and density functional perturbation theory (DFPT) [48], one can obtain the following Hamiltonian for electron-phonon coupled systems:

$$H_{\text{ep}} = H_0 + H_{\text{el-el}} + H_{\text{el-ph}}, \quad (1)$$

where

$$H_0 = \sum_{j,\mathbf{p},\sigma} \xi_{j\mathbf{p}} c_{j\mathbf{p}\sigma}^\dagger c_{j\mathbf{p}\sigma} + \sum_{\mathbf{q},\lambda} \omega_{\mathbf{q}\lambda} b_{\mathbf{q}\lambda}^\dagger b_{\mathbf{q}\lambda}, \quad (2)$$

$$H_{\text{el-el}} = \frac{1}{N} \sum_{\mathbf{q} \neq 0} \sum_{j,l,\mathbf{p}} V^c(\mathbf{q}) c_{j\mathbf{p}+\mathbf{q}\uparrow}^\dagger c_{j-\mathbf{p}-\mathbf{q}\downarrow}^\dagger c_{l-\mathbf{p}\downarrow} c_{l\mathbf{p}\uparrow}, \quad (3)$$

$$H_{\text{el-ph}} = \frac{1}{\sqrt{N}} \sum_{\mathbf{q} \neq 0, \lambda} \sum_{j, l, \mathbf{p}, \sigma} g_{\lambda}^{j\mathbf{p}+\mathbf{q}, l\mathbf{p}}(\mathbf{q}) (b_{\mathbf{q}\lambda} + b_{-\mathbf{q}\lambda}^{\dagger}) \times c_{j\mathbf{p}+\mathbf{q}\sigma}^{\dagger} c_{l\mathbf{p}\sigma}, \quad (4)$$

with  $c_{j\mathbf{p}\sigma}^{\dagger}$  ( $c_{j\mathbf{p}\sigma}$ ) being a creation (annihilation) operator of an electron with spin  $\sigma$  and momentum  $\mathbf{p}$  in the  $j$ -th band,  $\xi_{j\mathbf{p}}$  being an electron dispersion with respect to the Fermi level,  $b_{\mathbf{q}\lambda}^{\dagger}$  ( $b_{\mathbf{q}\lambda}$ ) being a creation (annihilation) operator of a phonon with momentum  $\mathbf{q}$  and mode  $\lambda$ ,  $\omega_{\mathbf{q}\lambda}$  being a phonon frequency,  $g_{\lambda}^{j\mathbf{p}+\mathbf{q}, l\mathbf{p}}(\mathbf{q})$  being an electron-phonon matrix element defined by Eq. (A8), and  $V^c$  being the bare electron-electron Coulomb interaction. Here we consider the Coulomb repulsion between electrons only for pairing channels explicitly since electron dispersion  $\xi_{j\mathbf{p}}$  already includes the contribution of the direct and exchange channel of the Coulomb interaction at the mean-field level [49]. Such a treatment is justified for weakly correlated systems like conventional superconductors.

The problem for conventional superconductivity is how to treat the Hamiltonian given by Eq. (1). Fortunately the Migdal theorem greatly simplifies complicated many-body problem of the electron-phonon coupled system through neglecting the vertex correction [39]. Within the framework of the Migdal-Eliashberg theory [39, 40], the self-energy is given by

$$\Sigma_{j\mathbf{p}}(i\omega_n) = -\frac{1}{N\beta} \sum_{l\mathbf{q}m} \tilde{V}_{j\mathbf{p}+\mathbf{q}, l\mathbf{p}}^{\text{ph}}(\mathbf{q}, i\omega_m) \times G_{l\mathbf{p}+\mathbf{q}}(i\omega_m + i\omega_n), \quad (5)$$

$$\Delta_{j\mathbf{p}}(i\omega_n) = \frac{1}{N\beta} \sum_{l\mathbf{q}m} \{ \tilde{V}_{j\mathbf{p}+\mathbf{q}, l\mathbf{p}}^{\text{ph}}(\mathbf{q}, i\omega_m) + \tilde{V}_{j\mathbf{p}+\mathbf{q}, l\mathbf{p}}^c(\mathbf{q}, i\omega_m) \} \times F_{l\mathbf{p}+\mathbf{q}}(i\omega_m + i\omega_n), \quad (6)$$

where  $j$  and  $l$  are the band indices,  $\Sigma_{j\mathbf{p}}(i\omega_n)$  and  $\Delta_{j\mathbf{p}}(i\omega_n)$  are the normal and the anomalous self-energies, and  $G_{j\mathbf{p}}(i\omega_n)$  and  $F_{j\mathbf{p}}(i\omega_n)$  are the electron normal and anomalous Green's functions. Here the band off-diagonal elements of the Green's function are neglected. If the density functional calculation is a good starting point for superconductors, the off-diagonal elements can be safely ignored.  $\tilde{V}^{\text{ph}}$  is the screened electron-electron interaction mediated by phonons. It is given by

$$\tilde{V}_{j\mathbf{p}+\mathbf{q}, l\mathbf{p}}^{\text{ph}}(\mathbf{q}, i\omega_m) = \sum_{\lambda} |\tilde{g}_{\lambda}^{j\mathbf{p}+\mathbf{q}, l\mathbf{p}}(\mathbf{q})|^2 D_{\mathbf{q}\lambda}(i\omega_m), \quad (7)$$

where  $\tilde{g}_{\lambda}^{j\mathbf{p}+\mathbf{q}, l\mathbf{p}}(\mathbf{q})$  and  $D_{\mathbf{q}\lambda}(i\omega_m)$  denote the screened electron-phonon matrix element and the phonon Green's function. Here  $\tilde{g}$  and  $D$  are screened quantities and should include the static screening effect by the electron polarization. On the other hand, in *ab initio* calculations based on density functional theory, calculated  $g$  and the phonon frequency already include such screening effects in the static level. Therefore, one can consider  $\tilde{g}$  in Eq. (7)

as  $g$  from DFPT and  $D$  as the free phonon Green's function defined by

$$D_{\mathbf{q}\lambda}(i\omega_m) = -\frac{2\omega_{\mathbf{q}\lambda}}{\omega_m^2 + \omega_{\mathbf{q}\lambda}^2}, \quad (8)$$

where  $\omega_{\mathbf{q}\lambda}$  is also calculated by DFPT.

The screened Coulomb interaction for the pairing channel,  $\tilde{V}_{j\mathbf{p}, l\mathbf{p}'}^c(i\omega_m) = \langle \psi_{j\mathbf{p}\uparrow} \psi_{j-\mathbf{p}\downarrow} | \epsilon^{-1}(i\omega_m) V^c | \psi_{l\mathbf{p}'\uparrow} \psi_{l-\mathbf{p}'\downarrow} \rangle$  is calculated through the symmetrized dielectric function [50],  $\tilde{\epsilon}_{\mathbf{G}\mathbf{G}'}$ , as

$$\tilde{V}_{j\mathbf{p}+\mathbf{q}, l\mathbf{p}}^c(i\omega_m) = \frac{4\pi}{\Omega} \sum_{\mathbf{G}\mathbf{G}'} \frac{\rho_{l\mathbf{p}}^{j\mathbf{p}+\mathbf{q}}(\mathbf{G}) \tilde{\epsilon}_{\mathbf{G}\mathbf{G}'}^{-1}(\mathbf{q}; i\omega_m) \{\rho_{l\mathbf{p}}^{j\mathbf{p}+\mathbf{q}}(\mathbf{G}')\}^*}{|\mathbf{q} + \mathbf{G}| |\mathbf{q} + \mathbf{G}'|}, \quad (9)$$

$$\tilde{\epsilon}_{\mathbf{G}\mathbf{G}'}(\mathbf{q}; i\omega_m) = \delta_{\mathbf{G}\mathbf{G}'} - \frac{4\pi}{\Omega} \frac{1}{|\mathbf{q} + \mathbf{G}|} \chi_{\mathbf{G}\mathbf{G}'}(\mathbf{q}; i\omega_m) \frac{1}{|\mathbf{q} + \mathbf{G}'|}. \quad (10)$$

Here,  $\chi$  is the polarization function,  $\mathbf{G}$  is the reciprocal lattice vector,  $\Omega$  is the volume of the unit cell and  $\rho_{l\mathbf{p}}^{j\mathbf{p}+\mathbf{q}}(\mathbf{G})$  is written as

$$\rho_{l\mathbf{p}}^{j\mathbf{p}+\mathbf{q}}(\mathbf{G}) = \int_{\Omega} d^3r \psi_{j\mathbf{p}+\mathbf{q}}^*(\mathbf{r}) e^{i(\mathbf{q}+\mathbf{G})\cdot\mathbf{r}} \psi_{l\mathbf{p}}(\mathbf{r}), \quad (11)$$

where  $\int_{\Omega}$  denotes the integration in the unit cell.

In this study, the screening is treated within the random phase approximation (RPA) [51]. In the RPA, the polarization function is given by the following equation:

$$\chi_{\mathbf{G}\mathbf{G}'}(\mathbf{q}; i\omega_m) = \frac{2}{\Omega} \sum_{\mathbf{p}} \sum_{j: \text{unocc}, l: \text{occ}} [\rho_{l\mathbf{p}}^{j\mathbf{p}+\mathbf{q}}(\mathbf{G})]^* \rho_{l\mathbf{p}}^{j\mathbf{p}+\mathbf{q}}(\mathbf{G}') \times \left\{ \frac{1}{i\omega_m - \xi_{j\mathbf{p}+\mathbf{q}} + \xi_{l\mathbf{p}}} - \frac{1}{i\omega_m + \xi_{j\mathbf{p}+\mathbf{q}} - \xi_{l\mathbf{p}}} \right\}. \quad (12)$$

Here the polarization function depends on the Matsubara frequency. However, we ignore this frequency dependence and treat the screened Coulomb interaction as a static repulsion between the paired electrons. One should notice that the structure of the Coulomb interaction along the frequency direction leads to an enhancement of  $T_c$  by the plasmon mechanism [52]. The inclusion of the frequency dependence for the screened Coulomb interaction is left as a future work.

For the calculation of  $T_c$ , the second order products of the anomalous quantities can be ignored. Therefore, the equations are linearized and the anomalous Green's function is reduced to the product of the normal Green's function and the anomalous self-energy like  $F_{j\mathbf{p}}(i\omega_n) = -G_{j\mathbf{p}}(i\omega_n) G_{j-\mathbf{p}}(-i\omega_n) \Delta_{j\mathbf{p}}(i\omega_n)$ .

In conventional calculations of  $T_c$  based on the ME theory, several approximations are introduced to simplify Eqs. (5) and (6) [53–55]. Since the pairing interaction works only for low energy states, we rewrite the

momentum sum as an energy integral assuming that DOS is constant around the Fermi level. For the Matsubara frequency sum, one introduces a cutoff frequency (of the order of the phonon energy scale) by replacing the Coulomb interaction  $\tilde{V}^c$  with the pseudo Coulomb potential  $\mu^*$  [56].  $\mu^*$  represents the retardation effect defined by

$$\mu^* = \frac{\mu}{1 + \mu \ln(\omega_{\text{el}}/\omega_c)}. \quad (13)$$

Here,  $\omega_{\text{el}}$  and  $\omega_c$  are the cutoff frequencies of the order of the electron and phonon energy scale, respectively, and  $\mu$  is the unrenormalized Coulomb potential written as

$$N(0)\mu = \frac{1}{N^2} \sum_{jl, \mathbf{p}\mathbf{q}} \tilde{V}_{j\mathbf{p}+\mathbf{q}, l\mathbf{p}}^c(0) \delta(\xi_{j\mathbf{p}+\mathbf{q}}) \delta(\xi_{l\mathbf{p}}), \quad (14)$$

where  $N(0)$  denotes the DOS at the Fermi level. With these approximations, the linearized version of Eqs. (5) and (6) are reduced to

$$Z(i\omega_n) = 1 + \frac{1}{\omega_n} \frac{\pi}{\beta} \sum_{n'} \lambda(i\omega_n - i\omega_{n'}) \text{sgn}(\omega_{n'}), \quad (15)$$

$$\phi(i\omega_n) = \frac{1}{Z(i\omega_n)} \frac{\pi}{\beta} \sum_{n'} \frac{\phi(i\omega_{n'})}{|\omega_{n'}|} \left\{ \lambda(i\omega_n - i\omega_{n'}) - \mu^* \right\}, \quad (16)$$

where  $Z(i\omega_n)$  and  $\phi(i\omega_n)$  denote the renormalization function and the gap function.  $\Sigma$  with prime denotes the summation with the frequency cutoff  $\omega_c$ .  $\lambda(i\omega_m)$  is the electron-phonon coupling

$$\lambda(z) = \int_0^\infty d\nu \frac{2\nu}{\nu^2 - z^2} \alpha^2 F(\nu), \quad (17)$$

and  $\alpha^2 F(\nu)$  is the Eliashberg function defined by

$$\alpha^2 F(\nu) = \frac{1}{N(0)} \sum_{jl, \mathbf{p}\mathbf{q}, \lambda} |g_\lambda^{j\mathbf{p}+\mathbf{q}, l\mathbf{q}}(\mathbf{q})|^2 \times \delta(\xi_{j\mathbf{p}+\mathbf{q}}) \delta(\xi_{l\mathbf{p}}) \delta(\nu - \omega_{\mathbf{q}\lambda}). \quad (18)$$

The Eliashberg function plays a central role in the conventional ME theory. If one knows  $\alpha^2 F$ ,  $T_c$  can be calculated with Eqs. (15) and (16) easily. In conventional calculations,  $\mu^*$  is not evaluated with Eqs. (13) and (14) but rather treated as an adjustable parameter [53–55].

While analytical formulation of the scheme considering the energy dependence of DOS is rather straightforward, actual calculation is numerically expensive. To mitigate the computational costs, we take momentum average of  $\tilde{V}^{\text{ph}}$  and  $\tilde{V}^c$  like  $\tilde{V}_{jl}^{\text{ph}}(\mathbf{q}, i\omega_m) = \langle \tilde{V}_{j\mathbf{p}+\mathbf{q}, l\mathbf{p}}^{\text{ph}}(\mathbf{q}, i\omega_m) \rangle_{\mathbf{p}}$  and  $\tilde{V}_{jl}^c(\mathbf{q}, i\omega_m) = \langle \tilde{V}_{j\mathbf{p}+\mathbf{q}, l\mathbf{p}}^c(\mathbf{q}, i\omega_m) \rangle_{\mathbf{p}}$ . In conventional superconductivity, this simplification could be a good approximation since the gap function is almost isotropic

and the complex momentum dependence is not important. For the phonon mediated interaction, this average is achieved by averaging the electron-phonon matrix element  $|g_\lambda^{jl}(\mathbf{q})|^2 = \langle |g_\lambda^{j\mathbf{p}+\mathbf{q}, l\mathbf{p}}(\mathbf{q})|^2 \rangle_{\mathbf{p}}$ . The averaged interaction is given by

$$\tilde{V}_{jl}^{\text{ph}}(\mathbf{q}, i\omega_m) = \sum_{\lambda} |g_\lambda^{jl}(\mathbf{q})|^2 D_{\mathbf{q}\lambda}(i\omega_m). \quad (19)$$

Then, the linearized equations are written as

$$\Sigma_{j\mathbf{p}}(i\omega_n) = -\frac{1}{N\beta} \sum_{l\mathbf{q}m} \tilde{V}_{jl}^{\text{ph}}(\mathbf{q}, i\omega_m) \times G_{l\mathbf{p}+\mathbf{q}}(i\omega_m + i\omega_n), \quad (20)$$

$$\Delta_{j\mathbf{p}}(i\omega_n) = -\frac{1}{N\beta} \sum_{l\mathbf{q}m} \{ \tilde{V}_{jl}^{\text{ph}}(\mathbf{q}, i\omega_m) + \tilde{V}_{jl}^c(\mathbf{q}, i\omega_m) \} \times G_{l\mathbf{p}+\mathbf{q}}(i\omega_n + i\omega_m) G_{l-\mathbf{p}-\mathbf{q}}(-i\omega_n - i\omega_m) \times \Delta_{l\mathbf{p}+\mathbf{q}}(i\omega_n + i\omega_m). \quad (21)$$

Based on this formulation, one can include the effect of energy dependent DOS on  $T_c$ .

Eq. (20) is solved with the Dyson equation:

$$G_{j\mathbf{p}}(i\omega_n) = \frac{1}{i\omega_n - \xi_{j\mathbf{p}} - \Sigma_{j\mathbf{p}}(i\omega_n)}, \quad (22)$$

by either the self-consistent (SC) or one-shot way. It should be noted that once we employ the constant DOS approximation, one cannot perform the SC calculation for the normal part. As mentioned above, this fact is ascribed to the neglect of the level shift function in the constant DOS approximation. On the other hand, in Eqs. (20) and (22), we fully include the effect of the level shift function, which comes from the antisymmetric part of the energy dependent DOS [55]. The level shift function and the self-consistency might be crucial for superconducting property when the DOS has a strong energy dependence around the Fermi level. Through the change of the normal Green's function, the pairing interaction in Eq. (21) could be modified [42, 44]. We will discuss this point in Sec. IV.

More practically, the momentum average of  $\tilde{V}^{\text{ph}}$  and the averaged electron-phonon matrix elements are calculated as

$$|g_\lambda^{jl}(\mathbf{q})|^2 = \frac{\sum_{\mathbf{p}} |g_\lambda^{j\mathbf{p}+\mathbf{q}, l\mathbf{p}}(\mathbf{q})|^2 \delta(\xi_{j\mathbf{p}+\mathbf{q}}) \delta(\xi_{l\mathbf{p}})}{\sum_{\mathbf{p}} \delta(\xi_{j\mathbf{p}+\mathbf{q}}) \delta(\xi_{l\mathbf{p}})}. \quad (23)$$

When the  $j$ - and  $l$ -th band are far away from the Fermi level and  $g_\lambda^{jl}(\mathbf{q})$  evaluated by (23) is smaller than a threshold value, the averaged matrix element is approximately calculated as

$$|g_\lambda^{jl}(\mathbf{q})|^2 = \frac{1}{N} \sum_{\mathbf{p}} |g_\lambda^{j\mathbf{p}+\mathbf{q}, l\mathbf{p}}(\mathbf{q})|^2. \quad (24)$$

As mentioned earlier, the advantage of solving Eqs. (20) and (21) is the inclusion of the energy dependence of DOS. Another advantage is that we can explicitly treat the retardation effect. In the calculation with the constant DOS approximation, it is in principle impossible to achieve the convergence with respect to the number of Matsubara frequencies. Since the gap function is almost constant in the high frequency region [53], the second term in the r.h.s. of Eq. (16) always diverges logarithmically for fixed  $\mu$  and sufficiently large number of Matsubara frequencies. To avoid this logarithmic divergence,  $\mu$  must be zero, which is totally unphysical. Therefore, one cannot reach a converged solution for non-empirically calculated  $\mu$  without introducing an adjustable electron energy cutoff [56]. Such a problem is mitigated in Eq. (21), since  $G_{j\mathbf{p}}(i\omega_n)G_{j-\mathbf{p}}(-i\omega_n)$  behaves as  $1/\omega_n^2$  in the high frequency limit. However, the numerical cost to achieve the convergence with respect to the Matsubara frequency is formidable, especially when  $T_c$  is low. This is because we need an extremely large number of Matsubara frequencies to cover the high frequency region. Fortunately, the  $T_c$ 's of sulfur hydrides are 30-200 K, which enables the Matsubara frequency grid to span a wide range of energy with a small number of grid points. We can therefore carry out the  $T_c$  calculation non-empirically—without introducing the adjustable parameters—with a feasible numerical cost.

In the calculation with the constant DOS approximation, one can also obtain the converged  $T_c$  with fixed  $\mu$  by introducing another cutoff frequency  $\omega_{el}$  for effective energy range of the Coulomb interaction, instead of  $\omega_c$ . With taking the isotropic limit and linearization, the momentum summation of the r.h.s. in Eq. (6) can be calculated analytically

$$\begin{aligned} & \frac{1}{N} \sum_{\mathbf{p}'l} G_{l\mathbf{p}'}(i\omega_{n'}) G_{l-\mathbf{p}'}(-i\omega_{n'}) \\ &= N(0) \int_{-\omega_{el}}^{\omega_{el}} d\xi \frac{1}{Z(i\omega_{n'})^2 \omega_{n'}^2 + \xi^2} \\ &= \frac{2N(0)}{Z(i\omega_{n'})\omega_{n'}} \arctan\left(\frac{\omega_{el}}{Z(i\omega_{n'})\omega_{n'}}\right). \end{aligned} \quad (25)$$

Thus, Eq. (16) becomes

$$\begin{aligned} \phi(i\omega_n) = \frac{1}{Z(i\omega_n)} \frac{\pi}{\beta} \sum_{n'} \frac{\phi(i\omega_{n'})}{|\omega_{n'}|} & \left\{ \lambda(i\omega_n - i\omega_{n'}) \right. \\ & \left. - \mu\eta_{n'}(\omega_{el}) \right\}, \end{aligned} \quad (26)$$

where  $\eta_n(\omega_{el})$  is the cutoff function defined by

$$\eta_n(\omega_{el}) = \frac{2}{\pi} \arctan\left(\frac{\omega_{el}}{Z(i\omega_n)|\omega_n|}\right). \quad (27)$$

Here, although the effective energy range is considerably different, both  $\lambda(i\omega_n)$  and  $\eta_n(\omega_{el})$  decay as a function of  $\omega_n$ . By combining Eqs. (15) and (26), one can calculate

$T_c$  with the fully non-empirically evaluated  $\mu$  if a large number of Matsubara frequencies is taken. Hereafter we call this treatment constant DOS ME theory.

## B. Allen-Heine-Cardona theory

The Allen-Heine-Cardona (AHC) theory is a perturbative approach to calculate ZPR from first-principles [58–61]. If the Hamiltonian  $H$  is perturbed by ion displacement  $u$  from its equilibrium position, it causes a shift of the electron energy. At the level of the second order perturbation, such a shift is given by

$$\begin{aligned} \delta\epsilon_{j\mathbf{p}} &= \frac{1}{2N} \sum_{\kappa\kappa',\mathbf{q}\lambda,\mu\nu} \sum_{l'l'} \sqrt{\frac{\hbar^2}{M_\kappa M_{\kappa'} \omega_{\mathbf{q}\lambda}^2}} \nabla_{l\kappa\mu} \nabla_{l'\kappa'\nu} \epsilon_{j\mathbf{p}} \\ &\quad \times e_{\kappa}^{\mu*}(\mathbf{q}\lambda) e_{\kappa'}^{\nu}(\mathbf{q}\lambda) e^{i\mathbf{q}\cdot(\mathbf{R}_{l'}-\mathbf{R}_l)} \left\{ \langle n_{\mathbf{q}\lambda} \rangle + \frac{1}{2} \right\} \\ &= \frac{1}{2N} \sum_{\kappa\kappa',\mathbf{q}\lambda,\mu\nu} \sqrt{\frac{\hbar^2}{M_\kappa M_{\kappa'} \omega_{\mathbf{q}\lambda}^2}} e_{\kappa}^{\mu*}(\mathbf{q}\lambda) e_{\kappa'}^{\nu}(\mathbf{q}\lambda) \\ &\quad \times \frac{\partial^2 \epsilon_{j\mathbf{p}}}{\partial u_{\mu\kappa}^*(\mathbf{q}) \partial u_{\nu\kappa'}(\mathbf{q})} \left\{ \langle n_{\mathbf{q}\lambda} \rangle + \frac{1}{2} \right\} \end{aligned} \quad (28)$$

where  $e_{\kappa}^{\mu}(\mathbf{q}\lambda)$  is the phonon polarization vector with momentum  $\mathbf{q}$  and mode  $\lambda$  defined through Eq. (A1),  $N$  is the number of  $\mathbf{q}$ -points,  $M_\kappa$  is the mass of the  $\kappa$ -th ion,  $\mathbf{R}_l$  is the position of the  $l$ -th unit cell,  $\langle n_{\mathbf{q}\lambda} \rangle$  is the Bose-Einstein distribution function, and  $\nabla_{l\kappa\mu} \nabla_{l'\kappa'\nu} \epsilon_{j\mathbf{p}}$  is the second order derivative of the Kohn-Sham energy [62] defined by

$$\begin{aligned} \nabla_{l\kappa\mu} \nabla_{l'\kappa'\nu} \epsilon_{j\mathbf{p}} &= \langle \psi_{j\mathbf{p}} | \nabla_{l\kappa\mu} \nabla_{l'\kappa'\nu} H | \psi_{j\mathbf{p}} \rangle \\ &\quad + \{ \langle \nabla_{l'\kappa'\nu} \psi_{j\mathbf{p}} | \nabla_{l\kappa\mu} H | \psi_{j\mathbf{p}} \rangle + \text{c.c.} \} \end{aligned} \quad (29)$$

with the Kohn-Sham orbital  $\psi_{j\mathbf{p}}$  and the Kohn-Sham energy  $\epsilon_{j\mathbf{p}}$ .  $\nabla_{l\kappa\mu}$  represents the derivative with respect to the  $\kappa$ -th ion position in the  $l$ -th unit cell for the  $\mu$ -th direction. The shift of the band energy coming from the first order and second order derivatives are called the Fan term [63] and Debye-Waller (DW) term [64], respectively. Here, the first order modulation of the Hamiltonian can be obtained by DFPT [48]. To evaluate the first order derivative of the wave function, one can utilize the Sternheimer approach [61, 62, 65] by separating the unoccupied manifold from the occupied space by

$$\begin{aligned} |\nabla_{l\kappa\mu} \psi_i\rangle &= - \sum_{j;\text{occ}} \frac{\langle \psi_j | \nabla_{l\kappa\mu} H | \psi_i \rangle}{\epsilon_i - \epsilon_j} |\psi_j\rangle \\ &\quad + P_{\text{unocc}} |\nabla_{l\kappa\mu} \psi_i\rangle, \end{aligned} \quad (30)$$

where the first term of the r.h.s. can be calculated by summing only over the occupied states, and the second term can be evaluated by standard DFPT [48]. Here  $P_{\text{unocc}}$  is projection to the unoccupied manifold. For the details about DFPT, see Appendix.

Compared with the first order derivative of the Hamiltonian, the second order derivative requires much more computational costs. The first order derivative can be treated as monochromatic perturbation [48], which means that for the calculation at momentum  $\mathbf{q}$ , it does not need information about other momenta  $\mathbf{q}' \neq \mathbf{q}$ . On the other hand, calculation for the second order derivative is not monochromatic and needs additional loop for momentum. Instead of calculating  $\langle \psi_{j\mathbf{p}} | \nabla_{l\kappa\mu} \nabla_{l'\kappa'\nu} H | \psi_{j\mathbf{p}} \rangle$  directly, one usually employs the acoustic sum rule and the rigid-ion approximation [58]. The acoustic sum rule represents the fact that the uniform displacements of the ions have no effect on the periodic system. It gives the constraint which connects the second order derivative with the first order through the following equation [62]:

$$\sum_{\kappa'} \frac{\partial^2 \epsilon_{j\mathbf{p}}}{\partial u_{\mu\kappa}^*(\mathbf{0}) \partial u_{\nu\kappa'}(\mathbf{0})} = 0. \quad (31)$$

On top of that, one can use the rigid-ion approximation. Namely, one can replace the second order derivative of the Hamiltonian with the first order derivative if the Hamiltonian is assumed to have the following form:

$$H_{\text{rigid-ion}} = K + \sum_{l\kappa} V_{l\kappa}(\mathbf{r} - \mathbf{R}_l - \mathbf{r}_\kappa) \quad (32)$$

with the electron kinetic energy  $K$  and the potential energy  $V_{l\kappa}$  caused by the  $\kappa$ -th ion in the  $l$ -th unit cell. Here  $\mathbf{r}_\kappa$  and  $\mathbf{R}_l$  represent the position of the  $\kappa$ -th ion and the  $l$ -th unit cell, respectively. It is apparent that  $\nabla_{l\kappa\mu} \nabla_{l'\kappa'\nu} H$  is equal to zero if  $\kappa \neq \kappa'$  as well as  $l \neq l'$ . This property leads to the following formula:

$$\begin{aligned} & \left\langle \psi_{j\mathbf{p}} \left| \frac{\partial^2 H}{\partial u_{\mu\kappa}^*(\mathbf{q}) \partial u_{\nu\kappa'}(\mathbf{q})} \right| \psi_{j\mathbf{p}} \right\rangle \\ &= \left\langle \psi_{j\mathbf{p}} \left| \frac{\partial^2 H}{\partial u_{\mu\kappa}^*(\mathbf{0}) \partial u_{\nu\kappa'}(\mathbf{0})} \right| \psi_{j\mathbf{p}} \right\rangle \delta_{\kappa\kappa'}. \end{aligned} \quad (33)$$

Combining Eqs. (29), (31) and (33), one can evaluate the shift of the electron band energy by

$$\delta \epsilon_{j\mathbf{p}} = \frac{1}{N} \sum_{\mathbf{q}\lambda} \frac{\partial \epsilon_{j\mathbf{p}}}{\partial n_{\mathbf{q}\lambda}} \left\{ \langle n_{\mathbf{q}\lambda} \rangle + \frac{1}{2} \right\}, \quad (34)$$

where  $\partial \epsilon_{j\mathbf{p}} / \partial n_{\mathbf{q}\lambda}$  is divided into two contributions

$$\frac{\partial \epsilon_{j\mathbf{p}}}{\partial n_{\mathbf{q}\lambda}} = \frac{\partial \epsilon_{j\mathbf{p}}^{(\text{Fan})}}{\partial n_{\mathbf{q}\lambda}} + \frac{\partial \epsilon_{j\mathbf{p}}^{(\text{DW})}}{\partial n_{\mathbf{q}\lambda}}, \quad (35)$$

and each term is written as

$$\begin{aligned} \frac{\partial \epsilon_{j\mathbf{p}}^{(\text{Fan})}}{\partial n_{\mathbf{q}\lambda}} &= \frac{\hbar}{2\omega_{\mathbf{q}\lambda}} \sum_{\kappa\kappa', \mu\nu} \sqrt{\frac{1}{M_\kappa M_{\kappa'}}} e_{\kappa}^{\mu*}(\mathbf{q}\lambda) e_{\kappa'}^{\nu}(\mathbf{q}\lambda) \\ &\times \left\{ \left\langle \frac{\partial \psi_{j\mathbf{p}}}{\partial u_{\kappa\mu}(\mathbf{q})} \left| \frac{\partial H}{\partial u_{\kappa'\nu}(\mathbf{q})} \right| \psi_{j\mathbf{p}} \right\rangle + \text{c.c.} \right\} \end{aligned} \quad (36)$$

$$\begin{aligned} \frac{\partial \epsilon_{j\mathbf{p}}^{(\text{DW})}}{\partial n_{\mathbf{q}\lambda}} &= -\frac{\hbar}{4\omega_{\mathbf{q}\lambda}} \sum_{\kappa\kappa', \mu\nu} \left\{ \frac{e_{\kappa}^{\mu*}(\mathbf{q}\lambda) e_{\kappa'}^{\nu}(\mathbf{q}\lambda)}{M_\kappa} + \frac{e_{\kappa'}^{\mu*}(\mathbf{q}\lambda) e_{\kappa}^{\nu}(\mathbf{q}\lambda)}{M_{\kappa'}} \right\} \\ &\times \left\{ \left\langle \frac{\partial \psi_{j\mathbf{p}}}{\partial u_{\kappa\mu}(\mathbf{0})} \left| \frac{\partial H}{\partial u_{\kappa'\nu}(\mathbf{0})} \right| \psi_{j\mathbf{p}} \right\rangle + \text{c.c.} \right\}. \end{aligned} \quad (37)$$

Here let us consider the validity of the rigid-ion approximation. In the Kohn-Sham system, the Hamiltonian does not have the form of Eq. (32) due to the Hartree and exchange-correlation potential. These potential terms depend on the electron density, and the electron density response to the displacement of one ion is affected by that of other ions. Therefore, the potential term cannot be expressed as the sum of the potentials of the individual ions. In spite of this fact, one can still expect that the rigid-ion approximation works well in three-dimensional materials as a consequence of the electronic screening [66]. The screening makes the range where the displacement of the different ions affects small and such short range effects is relevant only near the edge of the Brillouin zone (BZ). Since the volume of the edge regions becomes small in higher dimensional systems, one could safely apply the rigid-ion approximation to three-dimensional materials. For the DW contribution, this statement is confirmed in the case of diamond by comparing the result of the AHC theory with that of the frozen phonon approach [67].

In this study, we employ the AHC theory implemented in ABINIT [68] package for the evaluation of the ZPR. In the ABINIT calculation, we use the same pseudopotential used in the electronic and phononic structure calculations (see Sec. III).

### C. Self-consistent phonon theory

In this paper, we study how the anharmonicity changes the phonon dispersion and affects the self-energy of electrons, and consequently the superconducting  $T_c$ . Several *ab initio* approaches have been recently proposed for including anharmonic effects of phonons beyond quasi-harmonic level [69–73]. Here, we employ a deterministic method based on the self-consistent phonon (SCPH) theory [73, 74]. In our approach, the first-order effect of the frequency renormalization due to the quartic anharmonicity is treated nonperturbatively by solving the following SCPH equations:

$$\det \{ \omega^2 - \mathbf{U}_{\mathbf{q}} \} = 0, \quad (38)$$

$$U_{\mathbf{q}\lambda\lambda'} = \omega_{\mathbf{q}\lambda}^2 \delta_{\lambda\lambda'} + (2\omega_{\mathbf{q}\lambda})^{\frac{1}{2}} (2\omega_{\mathbf{q}\lambda'})^{\frac{1}{2}} \Pi_{\mathbf{q}\lambda\lambda'}. \quad (39)$$

Here the matrix  $\Pi_{\mathbf{q}}$  is the lowest-order phonon self-energy associated with the quartic terms defined as

$$\Pi_{\mathbf{q}\lambda\lambda'} = \sum_{\mathbf{q}_1, \lambda_1} \frac{\hbar \Phi(\mathbf{q}\lambda; -\mathbf{q}\lambda'; \mathbf{q}_1\lambda_1; -\mathbf{q}_1\lambda_1)}{8\sqrt{\omega_{\mathbf{q}\lambda}\omega_{\mathbf{q}\lambda'}\omega_{\mathbf{q}_1\lambda_1}}} [2\langle n_{\mathbf{q}_1\lambda_1} \rangle + 1]. \quad (40)$$

The tensor  $\Phi$  in the numerator represents the strength of the phonon-phonon coupling and can be calculated from the fourth-order interatomic force constants (IFCs) in real space as follows:

$$\begin{aligned} & \Phi(\mathbf{q}\lambda; -\mathbf{q}\lambda'; \mathbf{q}_1\lambda_1; -\mathbf{q}_1\lambda_1) \\ &= \frac{1}{N} \sum_{\{\kappa, \mu, l\}} \frac{e_{\kappa_1}^{\mu_1}(\mathbf{q}\lambda) e_{\kappa_2}^{\mu_2*}(\mathbf{q}\lambda') e_{\kappa_3}^{\mu_3}(\mathbf{q}_1\lambda_1) e_{\kappa_4}^{\mu_4*}(\mathbf{q}_1\lambda_1)}{\sqrt{M_{\kappa_1} M_{\kappa_2} M_{\kappa_3} M_{\kappa_4}}} \\ & \quad \times \Phi_{\mu_1\mu_2\mu_3\mu_4}(0\kappa_1; l_2\kappa_2; l_3\kappa_3; l_4\kappa_4) \\ & \quad \times e^{-i[\mathbf{q}\cdot\mathbf{R}_{l_2}-\mathbf{q}_1\cdot(\mathbf{R}_{l_3}-\mathbf{R}_{l_4})]}. \end{aligned} \quad (41)$$

By diagonalizing the Hermitian matrix  $\mathbf{U}_{\mathbf{q}}$ , one obtains phonon frequencies and corresponding eigenvectors modulated by fourth-order anharmonicity. Through this change of phonon frequencies and eigenvectors, the phonon self-energy  $\mathbf{\Pi}_{\mathbf{q}}$  is also updated. Therefore, Eqs. (38)–(41) need to be solved iteratively until a convergence is achieved with respect to anharmonic phonon frequencies. In this study, we neglect the mode off-diagonal elements of the phonon self-energy, i.e.  $\Pi_{\mathbf{q}\lambda\lambda'} \approx \Pi_{\mathbf{q}\lambda\lambda}\delta_{\lambda,\lambda'}$ , so that the phonon polarization vectors are not altered by anharmonic effects. The SCPH solution also includes the effect of zero-point motion [Eq. (40)], which is crucial for understanding anharmonic effects in sulfur hydrides under pressure [27].

To conduct the SCPH calculation, we need to calculate the fourth-order IFCs. For that purpose, we employ the real-space supercell approach, and anharmonic force constants are extracted from displacement-force training data sets prepared by DFT calculations. To reduce the number of independent IFCs and make the computation feasible, we make full use of space group symmetries and constraints due to the translational invariance [75]. Moreover, we employ the compressed sensing lattice dynamics method [76] for reliable and efficient estimation of force constants. An efficient implementation and more technical details of the present SCPH calculation can be found in Ref. [73].

### III. ELECTRONIC AND PHONONIC STRUCTURE

In previous works, several stable structures under high pressures are determined [18, 19, 22, 23, 25–27, 29, 36, 37]. Here we focus on the difference between  $\text{H}_2\text{S}$  and  $\text{H}_3\text{S}$ . In order to avoid the difficulty coming from structure instability near the transition point, we choose the pressures far from the critical pressure, which is around 180 GPa in  $\text{H}_3\text{S}$  and around 160 GPa in  $\text{H}_2\text{S}$ . For pressures close to the critical point, the electron-phonon coupling is strongly enhanced due to the structure instability, especially in the case of the second order phase transition in  $\text{H}_3\text{S}$  [19, 26, 27, 36], which considerably raises  $T_c$ . However, such enhancement of  $T_c$  might be an artifact of the harmonic approximation which cannot be justified in the vicinity of the phase transition since there are huge ion

oscillations toward other stable structure and one cannot assume the amplitude of these oscillations to be small. In Ref. [27], it is reported that anharmonicity strongly suppresses the electron-phonon coupling especially near the transition point for  $\text{H}_3\text{S}$ . Therefore, we hereafter choose 250 GPa for  $\text{H}_3\text{S}$  and 140 GPa for  $\text{H}_2\text{S}$ .

In order to study the superconducting property, first one should obtain the electronic and phononic structure of the target material precisely. For phonon frequencies and electron-phonon matrix elements, we utilize the framework of DFPT [48] as implemented in QUANTUM ESPRESSO [77]. Density functional calculations are performed within the generalized gradient approximation using the Perdew-Burke-Ernzerhof parameterization [78]. Atomic configurations and lattice constants are optimized by minimizing enthalpy under fixed pressures.

#### A. Electronic structure

In Fig. 1, we show the band dispersion of  $\text{H}_3\text{S}$  at 250 GPa and  $\text{H}_2\text{S}$  at 140 GPa. Under these pressures,  $Im\bar{3}m$  and  $P\bar{1}$  are the energetically most stable structures for  $\text{H}_3\text{S}$  and  $\text{H}_2\text{S}$ , respectively. The electron charge densities are obtained with  $16 \times 16 \times 16$  BZ mesh for  $Im\bar{3}m$  and  $12 \times 12 \times 8$  BZ mesh for  $P\bar{1}$ . The cutoff for the plane-wave energy is set to 100 Ry (80 Ry) for  $Im\bar{3}m$  ( $P\bar{1}$ ). We use the pseudopotential implemented based on the Troullier-Martins scheme [79]. In both Fig. 1 (a) and (b), the electronic bands far below the Fermi level have free electron like parabolic dispersion. However, near the Fermi level, there is a notable difference between  $Im\bar{3}m$  and  $P\bar{1}$  structures.

To clarify the difference of the electronic structures between  $Im\bar{3}m$ - $\text{H}_3\text{S}$  and  $P\bar{1}$ - $\text{H}_2\text{S}$ , the DOS calculated by the tetrahedron method [80] for these two structures are shown in Fig. 2. Near the Fermi level, there is a dip in the DOS for the  $P\bar{1}$  structure. In Fig. 2 (b) and (d), the enlarged views of the DOS are shown. In this energy scale, the DOS of the  $P\bar{1}$  structure is almost flat. On the other hand, there is a strong energy dependence of the DOS as a consequence of the vHs around the Fermi level for the  $Im\bar{3}m$  structure (Fig. 2 (b)). This narrow peak is a characteristic common feature of the DOS of the  $\text{H}_3\text{S}$  phases since one can also observe it in the  $R\bar{3}m$  structure [19], another stable structure stabilized under pressures around 180 GPa [19, 23, 26, 29].

The existence of the vHs is a good news for high- $T_c$  superconductivity since the large DOS at the Fermi level enhances the electron-phonon coupling [30]. However, the vHs makes it difficult to treat the superconductivity theoretically since the constant DOS approximation is not justified. This is the same situation as in the A15 compounds [41–45]. The constant DOS approximation overestimates the number of relevant states for superconductivity around the Fermi level and consequently  $T_c$  [25, 30, 42].



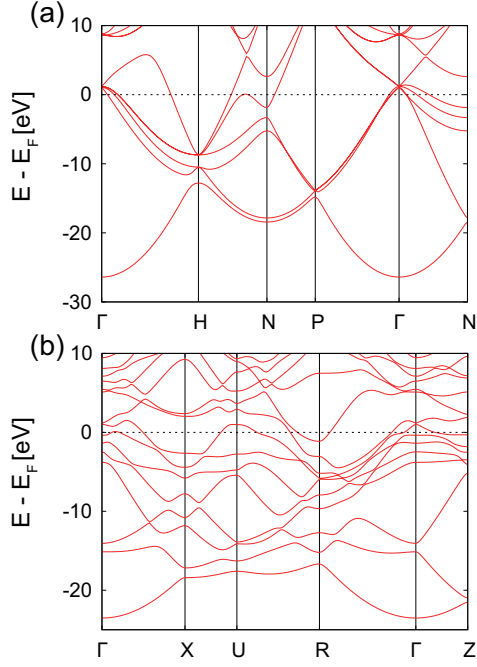


FIG. 1: Band structures of (a)  $Im\bar{3}m$ -H<sub>3</sub>S at 250 GPa and (b)  $P\bar{1}$ -H<sub>2</sub>S at 140 GPa along several high symmetry lines. Energy is measured from the Fermi level.

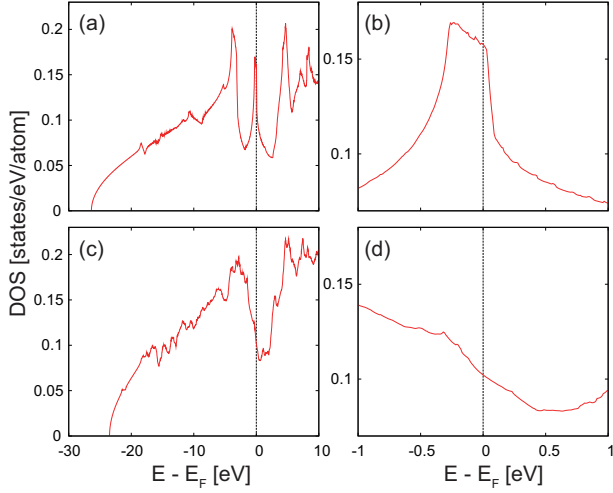


FIG. 2: Densities of states of (a)  $Im\bar{3}m$ -H<sub>3</sub>S and (c)  $P\bar{1}$ -H<sub>2</sub>S. (b) and (d) show the enlarged views of (a) and (c) around the Fermi level, respectively. The unit of the vertical axis is states per an atom. In (b), there is a sharp peak around the Fermi level and the peak width is comparable with the phonon energy scale, while (d) does not show any characteristic structures within the energy range of 1 eV.

## B. Phononic structure

Figure 3 shows the phonon dispersion relations for the two structures. For the linear response calculation, we use  $10 \times 10 \times 10$   $\mathbf{q}$ -mesh for  $Im\bar{3}m$ -H<sub>3</sub>S and  $12 \times 12 \times 8$   $\mathbf{q}$ -mesh for  $P\bar{1}$ -H<sub>2</sub>S, respectively. It is important to notice

that the typical phonon energy scale is extraordinarily high. In both Fig. 3 (a) and (b), the frequencies of the hardest modes are above  $1500 \text{ cm}^{-1}$ . This value is larger than phonon energies in simple metals by a factor of ten. The existence of these hard phonons is consistent with the prediction of high- $T_c$  superconductivity in hydrogen-rich compounds [5].

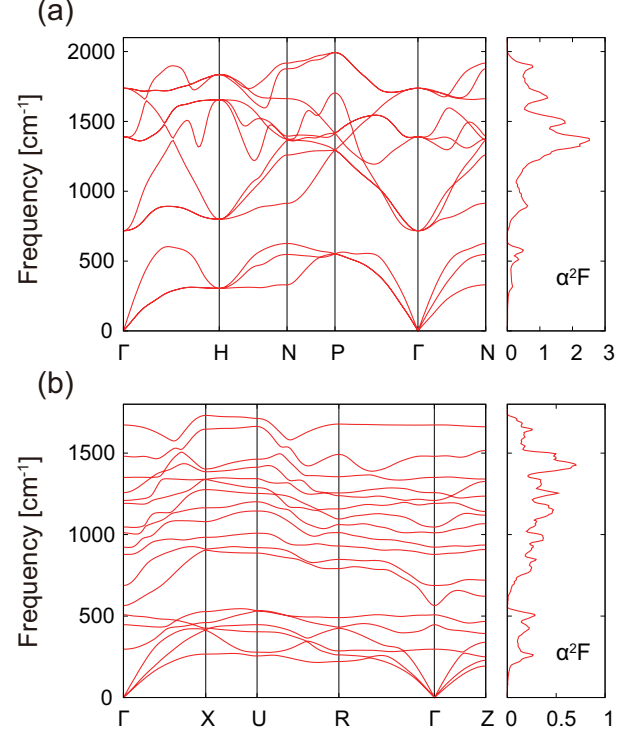


FIG. 3: Phonon dispersions and Eliashberg functions  $\alpha^2 F(\omega)$  in (a)  $Im\bar{3}m$ -H<sub>3</sub>S and (b)  $P\bar{1}$ -H<sub>2</sub>S.

To give more quantitative discussion about the energy scale of the phonons, we calculate  $\omega_{\text{ln}}$  defined by

$$\omega_{\text{ln}} = \exp \left\{ \frac{2}{\lambda} \int_0^\infty d\omega \frac{\alpha^2 F(\omega)}{\omega} \ln \omega \right\}, \quad (42)$$

where  $\lambda$  is the electron-phonon coupling constant defined by  $\lambda(0)$  in Eq. (17). The value of  $\omega_{\text{ln}}$  is 987 K ( $686 \text{ cm}^{-1}$ ) for the  $P\bar{1}$  structure and 1521 K ( $1057 \text{ cm}^{-1}$ ) for the  $Im\bar{3}m$  structure. These values are consistent with previous works [18, 19, 25–27]. Here it should be noticed that the scale of  $\omega_{\text{ln}}$  in H<sub>3</sub>S is comparable with the peak width of the DOS (Fig. 2 (b)). It clearly indicates that one should seriously consider the energy dependence of DOS to study the superconducting properties.

In addition to the high frequency phonons, the electron-phonon coupling also tells us that H<sub>3</sub>S should have higher  $T_c$  than H<sub>2</sub>S.  $\lambda$  takes the values of 0.86 in  $P\bar{1}$ -H<sub>2</sub>S, whereas it reaches 1.83 in  $Im\bar{3}m$ -H<sub>3</sub>S at 250 GPa with the first-order Hermite-Gaussian approximation [81] for the delta functions with the smearing width of 0.010 Ry. These values, which are calculated

using Eq. (17) with averaged electron-phonon matrix elements given by Eq. (23), are also consistent with previous studies [26, 27] ( $\lambda = 1.96$  in Ref. [27] with the Wannier interpolation for the electron-phonon matrix elements [82], and  $\lambda = 1.97$  in Ref. [26] with the optimized tetrahedron method [83] for the electron delta function in Eq. (18) in  $Im\bar{3}m$ -H<sub>3</sub>S). Therefore, the  $Im\bar{3}m$  structure is expected to have higher  $T_c$ . For other stable structures, such predictions of  $T_c$  also work qualitatively ( $R3m$  for H<sub>3</sub>S [19] and  $Cmca$  for H<sub>2</sub>S [18]).

Here we discuss why there is a huge difference in the electron-phonon coupling between H<sub>3</sub>S and H<sub>2</sub>S. One reason comes from the DOS. Since  $\lambda$  is roughly proportional to the DOS at the Fermi level, the electron-phonon coupling is enhanced by the large DOS (see Eq. (18)). From Fig. 2 (b) and (d), the DOS takes larger value in  $Im\bar{3}m$ -H<sub>3</sub>S than in  $P\bar{1}$ -H<sub>2</sub>S. Through the larger number of the available states around the Fermi level,  $\lambda$  in the  $Im\bar{3}m$  structure should become larger. Another point is the coupling strength between the electrons and the hydrogen vibration. It is shown that a half of  $\lambda$  comes from the low-lying sulfur vibrations (six modes below 500 cm<sup>-1</sup>) and the rest comes from the hydrogen oscillation in H<sub>2</sub>S [18]. On the other hand,  $\lambda$  in H<sub>3</sub>S originate mainly from the high frequency hydrogen oscillations. (70 % of  $\lambda$  is contributed from the hydrogen bond-stretching phonons [22]). Therefore, between H<sub>3</sub>S and H<sub>2</sub>S, there is a clear difference in the coupling of the electrons and the hydrogen oscillating phonons. It is pointed out that the larger  $\lambda$  in H<sub>3</sub>S is ascribed to the strong covalency of the hydrogen-sulfur bonding in Ref. [22].

#### IV. EFFECT OF STRONG EL-PH COUPLING ON THE VAN HOVE SINGULARITY AND SUPERCONDUCTIVITY

Using the electronic and phononic structure calculation in Sec. III, we perform the calculation of  $T_c$  for  $Im\bar{3}m$ -H<sub>3</sub>S and  $P\bar{1}$ -H<sub>2</sub>S based on the ME theory. As mentioned in Sec. I, for sulfur hydrides, we have to go beyond the constant DOS approximation employed in the previous calculations [18–20, 27, 29, 34, 36]. In this section, we will show that the energy dependence of the DOS is indeed crucial to describe the retardation effect properly. We also discuss how the self-consistency in the Green's function and self-energy is important for the quantitative estimation of  $T_c$ , which is not considered in the previous ME approaches with the constant DOS approximation. As is recently suggested by Ref. [28], in sulfur hydrides, the effect of ZPR on the spectral function can be significant. In this section, we also examine how ZPR affects superconductivity. Let us discuss these points one by one in the following subsections.

##### A. Energy dependence of DOS

In this subsection, we examine the importance of the energy dependence of the DOS for the accurate description of the retardation effect. With the strong energy dependence of the DOS at the Fermi level, it is expected that the constant DOS approximation is more problematic in H<sub>3</sub>S than in H<sub>2</sub>S. In order to see the effect of the energy dependence of the DOS on both compounds, we compare  $T_c$  calculated by Eqs. (15) and (26) with that by Eqs. (20) and (21). While the self-consistent dressed Green's function should be used in Eq. (21), here we employ the one-shot Green's function to focus on the effect of the energy dependence of the DOS on the retardation effect. It should be noticed that the self-consistency of the Green's function is not taken into account in the constant DOS approximation with Eqs. (15) and (26).

In the calculation based on the ME theory, the numerical cost to treat the Coulomb interaction is generally very expensive. This is because the Coulomb interaction is effective in the whole range of the band width, and thus it requires a large number of Matsubara frequencies. Therefore, one needs special care for the convergence with respect to the cutoff for the Matsubara frequency sum.

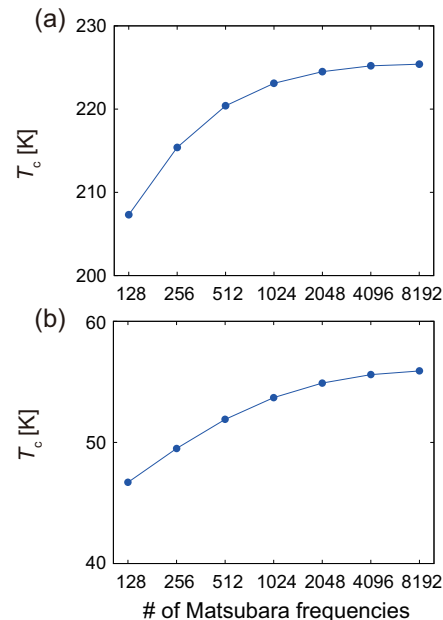


FIG. 4:  $T_c$  against the number of Matsubara frequencies for (a)  $Im\bar{3}m$ -H<sub>3</sub>S at 250 GPa and (b)  $P\bar{1}$ -H<sub>2</sub>S at 140 GPa within the constant DOS approximation.  $T_c$  is calculated for fixed  $\mu$  values of  $\mu = 0.32$  in (a) and  $\mu = 0.16$  in (b) evaluated with the RPA. The value of  $\omega_{el}$  is fixed at 20 eV for both structures.

Let us examine this problem in the calculation within and beyond the constant DOS approximation. As is discussed in Sec. II, we employ the RPA for the screened Coulomb interaction in Eq. (9). Following the argument by Migdal and Eliashberg [84], we neglect the frequency

dependence of the RPA screened Coulomb interaction:  $\tilde{V}^c(i\omega_n) = \tilde{V}^c(0)$ . In the constant DOS calculation with Eqs. (15) and (26), we introduce the averaged Coulomb potential  $\mu$  (Eq. (14)) and the adjustable cutoff  $\omega_{el}$ . One can calculate  $T_c$  with non-empirically evaluated  $\mu$  by utilizing  $\omega_{el}$  and the cutoff function. Figure 4 shows the summation cutoff dependence of  $T_c$  with fixed  $\mu$ . The value of  $\omega_{el}$  is set as 20 eV for the both structures. If the cutoff frequency  $\omega_{el}$  is fixed, we can obtain converged results with tractable numbers of Matsubara frequencies. It is also confirmed that the same results can be obtained by using Eq. (16) as the gap equation, where  $\mu^*$  is calculated by employing Eq. (13) with empirically selected  $\omega_{el}$  and  $\omega_c$ . Here, it should be noticed that this calculation is not fully *ab initio* because of the introduction of the cutoff for the effective Coulomb energy range. Although  $T_c$  is converged with fixed  $\omega_{el}$ , there still remains  $\omega_{el}$  dependence of  $T_c$  [85].

Now let us move on to the calculation beyond the constant DOS approximation to see how it solves the problem of the Matsubara frequency sum. In order to cover a wide energy range around the Fermi level, we include 7 (12) bands from the band bottom in  $Im\bar{3}m$ -H<sub>3</sub>S ( $P\bar{1}$ -H<sub>2</sub>S). As mentioned in Sec. II, Eq. (21) has natural convergent factor  $1/\omega_n^2$  in the frequency sum. Figure 5 shows the Matsubara frequency dependence of  $T_c$  in the calculation with energy dependent DOS. Here the normal Green's function is calculated by the one-shot treatment. A converged  $T_c$  is obtained with 512 Matsubara frequencies, slightly smaller number than that in the constant DOS calculation. This treatment has great advantage compared with the constant DOS ME theory since we can evaluate  $T_c$  by the fully non-empirical calculation based on the ME theory.

Finally, let us compare the results of the calculations with constant DOS and energy dependent DOS. We set the summation cutoff as 8192 frequencies in the constant DOS calculation for both structures, and 1024 and 2048 frequencies with energy dependent DOS for H<sub>3</sub>S and H<sub>2</sub>S, respectively. Figure 4 (a) shows that  $T_c$  is 225 K with the constant DOS approximation, and it decreases to 168 K without the constant DOS approximation for  $Im\bar{3}m$ -H<sub>3</sub>S (Fig. 5 (a)).  $T_c$  falls by 57 K (34 %) by considering the energy dependence of the DOS. It clearly indicates that the constant DOS approximation breaks down for  $Im\bar{3}m$ -H<sub>3</sub>S [25]. On the other hand, as seen in Fig. 4 (b) and 5 (b),  $T_c$  increases only by 10 K (15 %) in  $P\bar{1}$ -H<sub>2</sub>S (from 56 K with constant DOS to 66 K). By comparing the results in H<sub>3</sub>S and H<sub>2</sub>S, we can conclude that the existence of the narrow peak at the Fermi level must be treated carefully for the accurate estimate of  $T_c$ .

## B. Self-consistency for the normal Green's function

In this subsection, we discuss the importance of the self-consistency for the normal Green's function. We perform the calculation of  $T_c$  with both the one-shot and

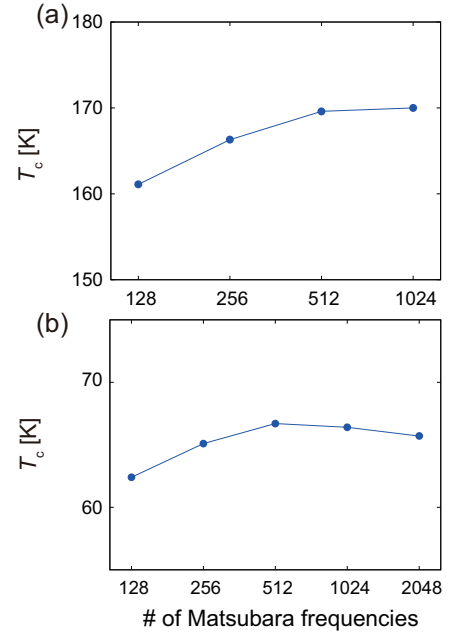


FIG. 5: Number of Matsubara frequencies dependence of  $T_c$  for (a)  $Im\bar{3}m$ -H<sub>3</sub>S at 250 GPa and (b)  $P\bar{1}$ -H<sub>2</sub>S at 140 GPa based on the ME theory with energy dependent DOS. The screened Coulomb interaction is evaluated with the RPA.

SC treatment for the normal Green's function. Figure 6 shows the mesh dependence of  $T_c$  in  $Im\bar{3}m$ -H<sub>3</sub>S. In both cases, convergence is already achieved with  $10 \times 10 \times 10$  mesh for the phonon calculation.

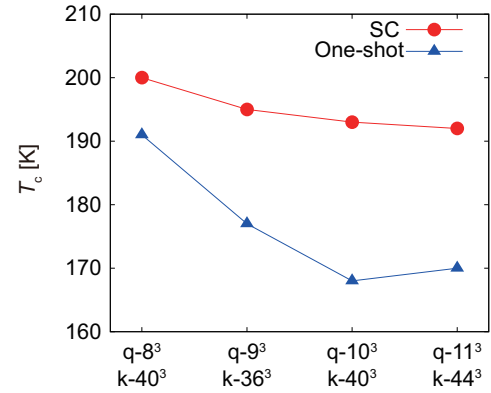


FIG. 6: Numerical convergence of  $T_c$  in  $Im\bar{3}m$ -H<sub>3</sub>S at 250 GPa. SC (red line) and One-shot (blue line) denote the self-consistent and one-shot calculations for the normal Green's function. The number of Matsubara frequencies is fixed at 1024.  $\mathbf{q}$  and  $\mathbf{k}$  represent the Brillouin zone sampling employed for the phonon dynamical matrix and the gap equation, respectively.

The results are listed in the second and third row in Table I. There is a clear difference of  $T_c$  in the case of  $Im\bar{3}m$ -H<sub>3</sub>S.  $T_c$  is enhanced by 25 K through the self-consistency of the normal Green's function. One can see that such enhancement of  $T_c$  is accompanied by the reduction of

the renormalization function. In Fig. 7, the momentum averaged renormalization function defined as

$$Z(i\omega_n) = 1 - \frac{\text{Im}\Sigma(i\omega_n)}{\omega_n} \quad (43)$$

is plotted as a function of the Matsubara frequency. In both cases,  $Z$  is suppressed and approached to one in the limit of large  $\omega_n$ . By contrast, near the minimum Matsubara frequency,  $Z$  in the one-shot treatment takes larger value than that in the SC calculation. There is a feedback effect in the self-consistent loop which mitigates the development of  $Z$ . The ratio of  $Z(i\pi/\beta)$  from the SC calculation to the equivalent from the one-shot calculation is 0.915 just below the transition temperature. The suppression of the renormalization function leads to the enhancement of  $T_c$  through the pairing interaction since  $Z$  denotes the mass enhancement of electrons.

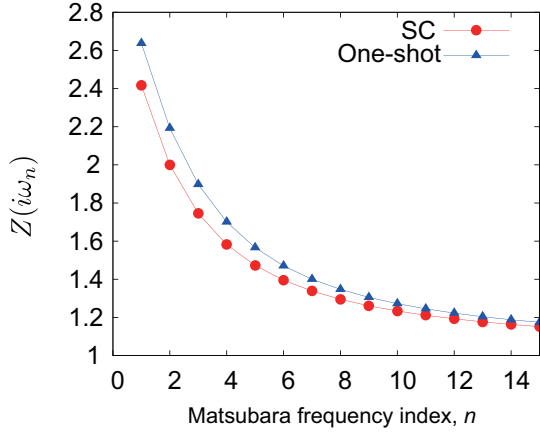


FIG. 7: Renormalization function  $Z(i\omega_n)$  as a function of the Matsubara frequency for  $Im\bar{3}m$ -H<sub>3</sub>S at 250 GPa. Here the Matsubara frequency is defined by  $\omega_n = (2n - 1)\pi/\beta$ . We choose the band crossing the Fermi level (the fifth band from the band bottom). SC (red line) and One-shot (blue line) denote the self-consistent and one-shot calculation for the normal Green's function, respectively. Plotted  $Z$  is calculated at 185 K in the SC calculation and 166 K in the one-shot calculation. Temperature dependence of  $Z$  is weak and irrelevant.

On the other hand,  $T_c$  does not show such huge variation in the case of  $P\bar{1}$ -H<sub>2</sub>S. Here we also calculate the ratio of  $Z(i\pi/\beta)$  for  $P\bar{1}$ -H<sub>2</sub>S and find that it is 0.987, which is much closer to unity than that of H<sub>3</sub>S in the  $Im\bar{3}m$  structure. This result indicates that the large suppression of the renormalization function by the self-consistency in H<sub>3</sub>S is related with the existence of the vHs. It reveals that the self-consistency is another important factor for accurate calculation of  $T_c$  when the DOS has strong energy dependence.

### C. Effect of zero-point motion on superconductivity

Figure 8 shows how the ZPR changes the band dispersions for H<sub>3</sub>S and H<sub>2</sub>S. Since the Fan term in the AHC theory (Eq. (36)) is already considered in the ME theory (Eq. (5)), hereafter we only take account of the contribution of the DW term (Eq. (37)) as ZPR [86]. For the calculation of the ZPR,  $18 \times 18 \times 18$  and  $14 \times 14 \times 8$  BZ sampling are employed for  $Im\bar{3}m$ -H<sub>3</sub>S and  $P\bar{1}$ -H<sub>2</sub>S, respectively. Temperature dependence of the band energy shift is small and only leads to slight changes in the calculation of  $T_c$ . In Fig. 8, there is apparently only small energy shifts by zero-point motion so that the ZPR in sulfur hydrides is not important. However, it is not necessarily the case since the energy shifts amount to a few hundred meV, which can generally have significant effects on superconductivity. Let us now take a closer look

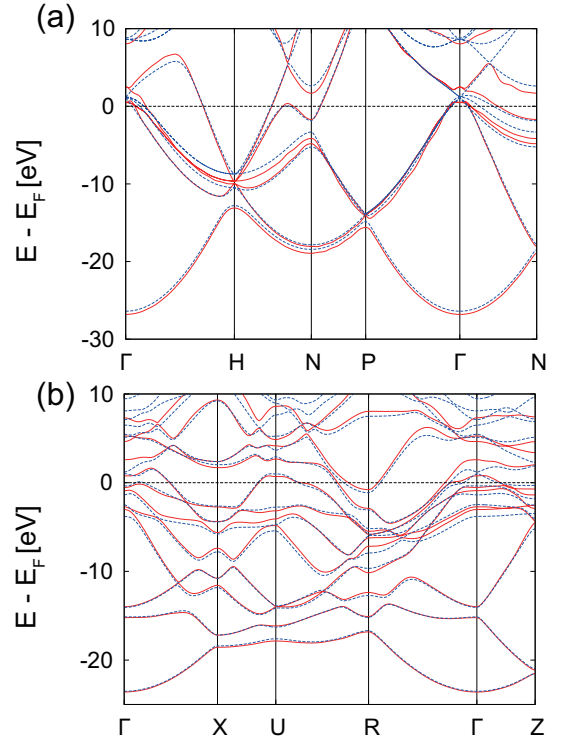


FIG. 8: Band dispersions with (red solid line) and without (blue broken line) ZPR for (a)  $Im\bar{3}m$ -H<sub>3</sub>S at 250 GPa and (b)  $P\bar{1}$ -H<sub>2</sub>S at 140 GPa. Band structures with ZPR are plotted by the Wannier interpolation.

at the DOS in the energy range relevant to superconductivity shown in Fig. 9. It clearly indicates that the DOS drastically changes due to the ZPR within the energy scale of phonons. It is interesting to note that there is an enhancement (suppression) of the DOS around the Fermi level for H<sub>3</sub>S (H<sub>2</sub>S).

With the ZPR, we calculate  $T_c$ . We treat the electron energy dispersion with the ZPR as an input for the ME calculation. The results are shown in the forth row in

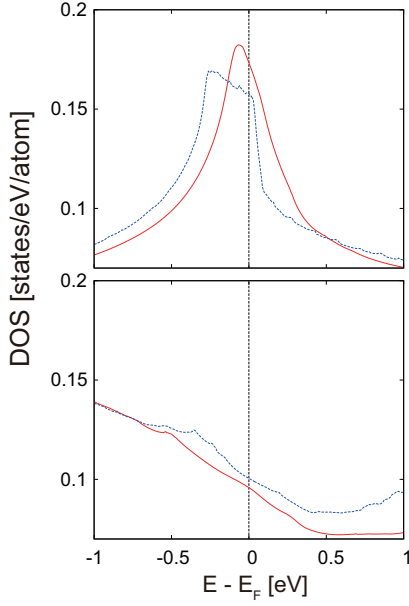


FIG. 9: Densities of states with (red solid line) and without (blue broken line) ZPR for (a)  $Im\bar{3}m$ -H<sub>3</sub>S at 250 GPa and (b)  $P\bar{1}$ -H<sub>2</sub>S at 140 GPa near the Fermi level.

Table I. In both  $Im\bar{3}m$ -H<sub>3</sub>S and  $P\bar{1}$ -H<sub>2</sub>S, there is a shift of  $T_c$  of the order of ten kelvin, although the direction is opposite. In the  $Im\bar{3}m$  structure,  $T_c$  gets raised by the ZPR, while it decreases in the  $P\bar{1}$  structure. Such shifts are naively consistent with the changes of the DOS shown in Fig. 9. In fact, we obtain  $\lambda = 2.06$  with ZPR and 1.83 without ZPR for  $Im\bar{3}m$ -H<sub>3</sub>S, and  $\lambda = 0.73$  with ZPR and 0.86 without ZPR for  $P\bar{1}$ -H<sub>2</sub>S.

Here it should be noted that there is a difference in the ratio of  $T_c$  shifts to the original values between H<sub>3</sub>S and H<sub>2</sub>S.  $T_c$  is raised by 9 K (5 %) in  $Im\bar{3}m$ -H<sub>3</sub>S, while there is a decrease of  $T_c$  by 19 K (30 %) in the  $P\bar{1}$ -H<sub>2</sub>S. This results indicate that, in H<sub>3</sub>S, the enhanced pairing interaction is smeared out within the energy scales of phonons and the effects of the attractive interaction are weaker than that expected by the value of  $\lambda$ . On the other hand, in H<sub>2</sub>S, since the DOS is reduced within the energy scales relevant to superconductivity, the effects of the reduction of the pairing interaction remain large even if the smearing effects are taken into account.

## V. ANHARMONICITY

We also examine the anharmonic effect on the calculation of  $T_c$ . In the previous study based on the constant DOS approximation for H<sub>3</sub>S [27], it has been shown that the anharmonicity makes the electron-phonon coupling weaker. Consequently,  $T_c$  dramatically decreases especially for the pressure near which the system undergoes the structural transition. Here we study the anharmonic effect in H<sub>2</sub>S and H<sub>3</sub>S considering the energy dependence

of the DOS. Figure 10 shows the phonon dispersion of  $Im\bar{3}m$ -H<sub>3</sub>S under 250 GPa and that of  $P\bar{1}$ -H<sub>2</sub>S under 140 GPa. Here we compare the results obtained by the SCPH theory (red solid lines) and by the harmonic approximation (blue dotted lines).

The SCPH calculations were conducted as follows: First, we performed first-principles molecular dynamics (FPMD) simulations at 300 K using  $3 \times 3 \times 3$  and  $3 \times 3 \times 2$  supercells for  $Im\bar{3}m$ -H<sub>3</sub>S and  $P\bar{1}$ -H<sub>2</sub>S, respectively, and extracted physically relevant atomic configurations in every 50 MD steps ( $\sim 24.2$  fs). For the sampled snapshots, we then added random displacements to each atom to reduce the cross-correlation inherent in the FPMD trajectories [76]. For H<sub>3</sub>S (H<sub>2</sub>S), we prepared 40 (250) displacement patterns and calculated forces for each configuration using QUANTUM ESPRESSO. Next, using the displacement-force training data, we estimated anharmonic IFCs by the least absolute shrinkage and selection operator (LASSO) method. Here, anharmonic IFCs up to the sixth order were included in the anharmonic lattice model [75] to improve the prediction accuracy. The total number of independent parameters was as large as 9000 (28000) for H<sub>3</sub>S (H<sub>2</sub>S), from which a sparse solution having  $\sim 3700$  ( $\sim 16000$ ) non-zero parameters was obtained by LASSO with a regularization parameter determined by cross-validation. The accuracy of the estimated IFCs was checked by applying them to independent test configurations, where the interatomic forces predicted by the model showed good agreements with DFT values for both H<sub>3</sub>S and H<sub>2</sub>S. Finally, we solved the SCPH equation [Eqs. (38)-(41)] at 0 K using the quartic IFCs estimated by LASSO and the harmonic dynamical matrices calculated by DFPT. The SCPH equation was solved using  $5 \times 5 \times 5$   $\mathbf{q}$ -mesh for H<sub>3</sub>S and  $3 \times 3 \times 2$   $\mathbf{q}$ -mesh for H<sub>2</sub>S, and the same mesh densities were employed for the  $\mathbf{q}_1$  point in Eq. (40). Doubling the  $\mathbf{q}_1$ -mesh points along each direction did not change the results for both systems, indicating the finite size effect is not significant at the selected pressures. The anharmonic correction to the dynamical matrix  $\Delta \mathbf{D}(\mathbf{q}) = \mathbf{D}^{\text{SCPH}}(\mathbf{q}) - \mathbf{D}^{\text{DFPT}}(\mathbf{q})$  was transformed into the real-space force constants  $\Delta \Phi_{\mu\nu}(0\mathbf{k}; l'\mathbf{k}')$ , from which anharmonic phonon frequencies at denser  $\mathbf{q}$  points were obtained by interpolation.

We see that the anharmonicity changes the phonon dispersion, especially for phonons whose frequencies are higher than  $\sim 500 \text{ cm}^{-1}$  [27]. As a result, the electron-phonon coupling is weakened from 2.06 to 1.86 (1.83 to 1.64) for the H<sub>3</sub>S, and from 0.73 to 0.64 (0.86 to 0.75) for the H<sub>2</sub>S when the ZPR is considered (neglected) [87]. By contrast,  $\omega_{\text{ln}}$  stays nearly unchanged by the anharmonicity (from 1521 K (987 K) with the harmonic approximation, to 1515 K (1034 K) with the anharmonicity for  $Im\bar{3}m$ -H<sub>3</sub>S ( $P\bar{1}$ -H<sub>2</sub>S)).

The modification of the phonon frequencies lowers  $T_c$ . It is confirmed by the calculation of  $T_c$  based on the self-consistent ME theory with the zero-point renormalization. As listed in Table I, the values of  $T_c$  become 181 K in  $Im\bar{3}m$ -H<sub>3</sub>S, and 34 K in  $P\bar{1}$ -H<sub>2</sub>S. The anhar-



TABLE I: Calculated  $T_c$  for  $Im\bar{3}m$ -H<sub>3</sub>S at 250 GPa and  $P\bar{1}$ -H<sub>2</sub>S at 140 GPa with different methods. The first row shows  $T_c$  with the constant DOS approximation. One-shot and SC denote the one-shot calculation and self-consistent calculation for the normal Green's function. ZPR and AH denote the zero-point renormalization for the electron dispersion, and the anharmonicity for the phonon frequency, respectively.

	$Im\bar{3}m$ -H <sub>3</sub> S	$P\bar{1}$ -H <sub>2</sub> S
const. DOS	225 K	56 K
One-shot	168 K	66 K
SC	193 K	63 K
SC + ZPR	202 K	44 K
SC + ZPR + AH	181 K	34 K

monicity reduces  $T_c$  by 21 K (12%) in the  $Im\bar{3}m$  structure [88], and 10 K (29%) in the  $P\bar{1}$  structure. Here, the change in  $T_c$  by the anharmonicity is the same order as the shift by both the ZPR and the feedback effect in the self-consistent calculation. This result confirms that the anharmonicity is also important factors in the calculation of  $T_c$ , as well as the ZPR and the self-consistency of the normal self-energy.

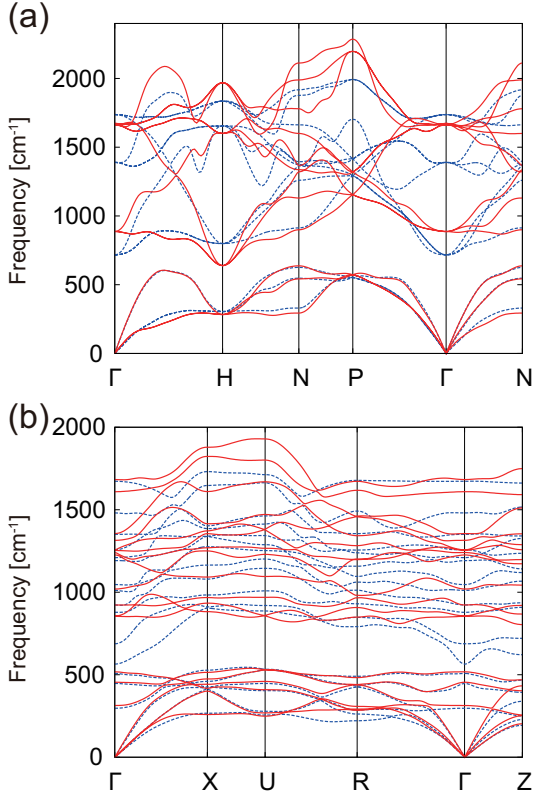


FIG. 10: Phonon dispersion relation for (a)  $Im\bar{3}m$ -H<sub>3</sub>S at 250 GPa and (b)  $P\bar{1}$ -H<sub>2</sub>S at 140 GPa. The red solid line shows the dispersion considering the anharmonic effect within the SCPH theory, and the blue broken line shows the result within the harmonic approximation.

## VI. VERTEX CORRECTION

In the ME theory, the vertex function is assumed to be dominated by the lowest order vertex, which is equal to one, and higher order contributions are neglected. In order to obtain the quantitative criterion for the justification of the ME theory, we evaluate the lowest order vertex correction [84]. Here the lowest order vertex correction  $\Gamma_{j\mathbf{p}+\mathbf{q},l\mathbf{p}}^{(1)\lambda}(i\omega_n + i\omega_m, i\omega_n)$  is given by

$$\begin{aligned} & g_{\lambda}^{j\mathbf{p}+\mathbf{q},l\mathbf{p}}(\mathbf{q}) \Gamma_{j\mathbf{p}+\mathbf{q},l\mathbf{p}}^{(1)\lambda}(i\omega_n + i\omega_m, i\omega_n) \\ &= \frac{-1}{N\beta} \sum_{\mathbf{k},n'} \sum_{\lambda',j',l'} g_{\lambda}^{l'\mathbf{k}+\mathbf{q},j'\mathbf{k}}(\mathbf{q}) G_{l'\mathbf{k}}(i\omega_{n'}) G_{j'\mathbf{k}+\mathbf{q}}(i\omega_{n'} + i\omega_m) \\ &\times g_{\lambda'}^{j\mathbf{p}+\mathbf{q},j'\mathbf{k}+\mathbf{q}}(\mathbf{p}-\mathbf{k}) D_{\mathbf{p}-\mathbf{k}\lambda'}(i\omega_n - i\omega_{n'}) g_{\lambda'}^{l'\mathbf{k},l\mathbf{p}}(\mathbf{k}-\mathbf{p}). \end{aligned} \quad (44)$$

If the ME theory is justified, at least the lowest order correction should be small compared with one.

The lowest order vertex correction has a complicated dependence on momenta, band indices, frequencies, and phonon modes. To simplify the evaluation, we here employ several approximations for Eq. (44) as follows: First, phonons are treated as a single Einstein phonon, which does not have any momentum dependence. Then the phonon Green's function is replaced by

$$D(i\omega_m) = -\frac{2\langle\omega\rangle}{\omega_m^2 + \langle\omega\rangle^2}, \quad (45)$$

where  $\langle\omega\rangle$  is the averaged phonon frequency. In addition, we ignore the momentum and band index dependence of the electron-phonon matrix element, and replace it with the averaged electron-phonon matrix element  $\langle g \rangle$ . In this case, we could express the averaged electron-phonon matrix element  $\langle g \rangle$  and averaged phonon frequency  $\langle\omega\rangle$  in terms of the electron-phonon coupling  $\lambda$  through the following relation:

$$\lambda = \frac{2N(0)\langle g \rangle^2}{\langle\omega\rangle}. \quad (46)$$

With these substitution, the vertex correction only has the  $\mathbf{q}$ -momentum and the Matsubara frequencies dependence, and can be written by

$$\begin{aligned} \Gamma_{\mathbf{q}}^{(1)}(i\omega_n + i\omega_m, i\omega_n) &= \frac{\lambda}{N(0)} \frac{1}{N\beta} \sum_{\mathbf{k},n'} \sum_{j',l'} \frac{\langle\omega\rangle^2}{\omega_{n-n'}^2 + \langle\omega\rangle^2} \\ &\times G_{l'\mathbf{k}}(i\omega_{n'}) G_{j'\mathbf{k}+\mathbf{q}}(i\omega_{n'} + i\omega_m). \end{aligned} \quad (47)$$

In Eq. (47), the averaged electron-phonon matrix element  $\langle g \rangle$  does not appear explicitly but has a contribution only through  $\lambda$ . Therefore, we do not need to evaluate  $\langle g \rangle$  explicitly. Finally, the electron Green's function is replaced by the non-interacting one.

In the practical calculation, we focus on diagonal elements of the vertex correction in terms of the Matsubara

frequency dependence by setting  $\omega_m$  as 0 and evaluate Eq. (47) at  $\omega_n = \pi/\beta$ . In the case of  $Im\bar{3}m$ -H<sub>3</sub>S ( $P\bar{1}$ -H<sub>2</sub>S), we consider 15 (25) bands and use  $100 \times 100 \times 100$  ( $48 \times 48 \times 32$ )  $\mathbf{k}$ -mesh for the sum in the r.h.s. of Eq. (47). Since the phonon Green's function works as a convergence factor for the Matsubara frequency sum, 25 (100) Matsubara frequencies are enough to obtain converged results. Here, temperature is set as 200 K (50 K) for  $Im\bar{3}m$ -H<sub>3</sub>S ( $P\bar{1}$ -H<sub>2</sub>S). For the phonon Green's function, the  $\omega_n$  defined by Eq. (42) is used as the averaged phonon frequency  $\langle\omega\rangle$ . The ZPR and anharmonicity are neglected in this calculation.

By using Eq. (47) with  $20 \times 20 \times 20$  ( $12 \times 12 \times 8$ )  $\mathbf{q}$ -mesh for  $Im\bar{3}m$ -H<sub>3</sub>S ( $P\bar{1}$ -H<sub>2</sub>S), we estimate the lowest order vertex correction. Here, we use  $\Delta\Gamma^{(1)}$  calculated by averaging  $\Gamma_{\mathbf{q}}^{(1)}(i\omega_n, i\omega_n)$  over  $\mathbf{q}$  as a measure of the vertex correction, and  $\Delta\Gamma^{(1)}$  is estimated to be  $-0.22$  ( $-0.12$ ). We then calculate  $T_c$  by replacing the square of the electron-phonon matrix element and the screened Coulomb interaction with  $(1 + \Delta\Gamma^{(1)})|g_{\lambda}^{jl}(\mathbf{q})|^2$  and  $(1 + \Delta\Gamma^{(1)})\tilde{V}^c(\mathbf{q}, i\omega_m)$ , respectively [89]. We found that the vertex correction changes  $T_c$  by  $-34$  K ( $-18\%$ ) for  $Im\bar{3}m$ -H<sub>3</sub>S and  $-13$  K ( $-20\%$ ) for  $P\bar{1}$ -H<sub>2</sub>S. We see that the impact of the vertex correction on  $T_c$  is similar to that of ZPR and anharmonicity. If we take account of the fact that the plasmon effect enhances  $T_c$  in  $Im\bar{3}m$ -H<sub>3</sub>S by 20 K [26], we see that the present non-empirical calculation shows an excellent agreement with the experiment (see Table II, where the experimental  $T_c$  is compared with those in the present and previous studies).

It was shown for a simple model system that the lowest order vertex correction is negative in the static limit of  $\omega_m \rightarrow 0$  with finite  $\mathbf{q}$  [90]. Our results are consistent with these previous studies. On the other hand, it was also reported that the vertex correction becomes positive and contributes to the enhancement of  $T_c$  in the dynamical limit ( $\mathbf{q} = 0$  with finite  $\omega_m$ ). Since these static and dynamical regions in the  $\mathbf{q}$ - $\omega_m$  plane are approximately separated by a line of  $v_F|\mathbf{q}| \approx \omega_m$  where  $v_F$  is the Fermi velocity, the net contribution of the vertex correction depends on the energy scale of phonons and  $v_F|\mathbf{q}|$ . Our results give the lower bound of  $T_c$  corrected by the inclusion of the vertex function in that we take the limit of  $\omega_m \rightarrow 0$ . Thus especially for H<sub>3</sub>S having small  $v_F$  around vHs, the effect of the vertex correction may be overestimated in the present calculation, since the dynamical contribution can be relevant [91]. Further study for the vertex function based on a more sophisticated treatment [92] is also an interesting future problem.

## VII. SUMMARY

One of the most characteristic features in the electronic structure of H<sub>3</sub>S under high pressures is the existence of the vHs around the Fermi level, which is absent for the low  $T_c$  phases of H<sub>2</sub>S. While it has been known that it is crucial to take account of the energy dependence of the

vHs for accurate estimate of  $T_c$ , in the previous *ab initio* calculation based on the ME theory, the constant DOS approximation has been employed.

In this study, we performed a self-consistent ME analysis in which we explicitly considered the electronic structure over 40 eV around the Fermi level. Since  $T_c$ 's of sulfur hydrides are extremely high, with a reasonably large number of Matsubara frequencies (up to  $\sim 1000$ ) in the Eliashberg equation, the retardation effect of the Coulomb interaction could be directly treated. By calculating  $T_c$  of H<sub>3</sub>S (H<sub>2</sub>S), in which vHs are present (absent) near the Fermi level, we showed that the constant DOS approximation employed so far seriously overestimates (underestimates)  $T_c$  by  $\sim 60$  K ( $\sim 10$  K). In addition, we discussed how the self-energy due to the strong electron-phonon coupling affects the vHs and  $T_c$ , especially focusing on (1) the feedback effect in the self-consistent calculation of the self-energy, (2) the effect of the ZPR, and (3) the effect of the changes in the phonon frequencies due to the strong anharmonicity. We showed that the effect of (1)-(3) on  $T_c$  is about 10-30 K for both H<sub>3</sub>S and H<sub>2</sub>S, and eventually  $T_c$  is estimated to be 181 K for H<sub>3</sub>S, and 34 K for H<sub>2</sub>S. These results explain the pressure dependence of  $T_c$  observed in the experiment if it is considered that high- (low-)  $T_c$  superconductivity under pressures higher (lower) than  $\sim 150$  GPa is attributed to that of H<sub>3</sub>S (H<sub>2</sub>S). Finally, we evaluated the lowest order vertex correction and we found that its impact on  $T_c$  is as large as that of ZPR and anharmonicity.

## Acknowledgments

We thank Mitsuaki Kawamura, Masatoshi Imada, Yohei Yamaji, and Yasutami Takada for fruitful discussions. We also would like to thank Emmanuele Cappelluti for enlightening comments about the vertex correction. This work are financially supported by JST, PRESTO and JSPS KAKENHI Grant Numbers 15K20940 (R.Ak.) and 15H03696 (T.K. and R.Ar.). This work is partially supported by Tokodai Institute for Element Strategy (TIES) funded by MEXT Elements Strategy Initiative to Form Core Research Center and by the Computational Material Science Initiative (CMSI).

## Appendix A: Density functional perturbation theory

In solids, the phonon frequencies are calculated by the following equation:

$$\sum_{\nu\kappa'} D_{\mu\kappa,\nu\kappa'}(\mathbf{q}) e_{\kappa'}^{\nu}(\mathbf{q}\lambda) = \omega_{\mathbf{q}\lambda}^2 e_{\kappa}^{\mu}(\mathbf{q}\lambda) \quad (\text{A1})$$

with a momentum  $\mathbf{q}$ , ion index  $\kappa$ , and displacement direction  $\mu, \nu = \{x, y, z\}$ . This equation is an eigenvalue problem for  $3n \times 3n$  matrix  $D(\mathbf{q})$  with  $n$  being the number of atoms. Therefore the square root of the eigenvalue

TABLE II: Comparison of  $T_c$  in  $Im\bar{3}m$ -H<sub>3</sub>S with previous studies. Except for the row of Flores-Livas *et al.* [25], pressure is set to be 250 GPa. The first and second rows show  $T_c$  calculated with an adjustable parameter  $\mu^*$ . Both the third and forth rows refer to calculations of  $T_c$  based on SCDF. Akashi *et al.* [26] has revealed that the plasmon effect enhances  $T_c$  by  $\sim 20$  K in  $Im\bar{3}m$ -H<sub>3</sub>S. If such a contribution is added to our calculation (Table I) with the static vertex correction, the resulting  $T_c$  shows an excellent agreement with the experimental value as show in the seventh row.

	$T_c$ [K]	Remark
Duan <i>et al.</i> [19]	184	McMillan ( $\mu^* = 0.13$ )
Errea <i>et al.</i> [27]	190	const. DOS ME ( $\mu^* = 0.16$ ) + anharmonicity
Flores-Livas <i>et al.</i> [25]	180	SCDFT ( $P = 200$ GPa)
Akashi <i>et al.</i> [26]	211	SCDFT + plasmon different approximation with Ref. [25]
This work	181	
	$\sim 147$	static vertex correction $\sim -34$ K
	$\sim 167$	plasmon effect $\sim +20$ K
Experiment [15]	$\sim 160$	extrapolation of Fig. 2 of Ref. [15]

$\omega_{\mathbf{q}\lambda}$  and the polarization vector  $e_{\kappa}^{\mu}(\mathbf{q}\lambda)$  have mode index  $\lambda$ , which runs  $1\dots 3n$ . The matrix  $D(\mathbf{q})$  is called the dynamical matrix and given by

$$D_{\mu\kappa,\nu\kappa'}(\mathbf{q}) = \frac{1}{\sqrt{M_{\kappa}M_{\kappa'}}}\Phi_{\mu\kappa,\nu\kappa'}(\mathbf{q}) \quad (\text{A2})$$

where  $M_{\kappa}$  is the mass of the  $\kappa$ -th ion,  $\Phi_{\mu\kappa,\nu\kappa'}(\mathbf{q})$  is the interatomic force constant

$$\Phi_{\mu\kappa,\nu\kappa'}(\mathbf{q}) = \frac{1}{N} \frac{\partial^2 E(\{\mathbf{R}_{\kappa}^0\})}{\partial u_{\mu\kappa}^*(\mathbf{q}) \partial u_{\nu\kappa'}(\mathbf{q})} \quad (\text{A3})$$

with the Born-Oppenheimer energy surface  $E(\{\mathbf{R}_{\kappa}^0\})$ , the number of  $\mathbf{q}$ -points  $N$ , the equilibrium positions of the ions  $\{\mathbf{R}_{\kappa}^0\}$ , and the displacement of the ions  $u$ .

Derivatives of the Born-Oppenheimer energy surface can be written as

$$\begin{aligned} \frac{\partial^2 E(\{\mathbf{R}_{\kappa}^0\})}{\partial u_{\mu\kappa}^*(\mathbf{q}) \partial u_{\nu\kappa'}(\mathbf{q})} &= \int \frac{\partial^2 V_{ie}(\mathbf{r})}{\partial u_{\mu\kappa}^*(\mathbf{q}) \partial u_{\nu\kappa'}(\mathbf{q})} n(\mathbf{r}) d^3r \\ &+ \int \frac{\partial V_{ie}(\mathbf{r})}{\partial u_{\mu\kappa}^*(\mathbf{q})} \frac{\partial n(\mathbf{r})}{\partial u_{\nu\kappa'}(\mathbf{q})} d^3r \\ &+ \frac{\partial^2 U_{ii}}{\partial u_{\mu\kappa}^*(\mathbf{q}) \partial u_{\nu\kappa'}(\mathbf{q})} \end{aligned} \quad (\text{A4})$$

with the electron density  $n(\mathbf{r})$ , the ionic potential  $V_{ie}(\mathbf{r})$  and the ion-ion interaction energy  $U_{ii}$ . This formulation can be used for the calculation of the dynamical matrix.

To evaluate Eq. (A4), one needs the response of the electron density to the ionic displacement. With the Kohn-Sham orbital  $\psi_i$ , the electron density response  $\partial n(\mathbf{r})/\partial u_{\mu\kappa}(\mathbf{q})$  is given by

$$\frac{\partial n(\mathbf{r})}{\partial u_{\mu\kappa}(\mathbf{q})} = 4\text{Re} \sum_{i;\text{occ}} \psi_i^*(\mathbf{r}) \frac{\partial \psi_i(\mathbf{r})}{\partial u_{\mu\kappa}(\mathbf{q})}, \quad (\text{A5})$$

where the derivative of the wave function can be written as

$$(H_{\text{KS}} - \epsilon_i) \left| \frac{\partial \psi_i}{\partial u_{\mu\kappa}(\mathbf{q})} \right\rangle = - \left( \frac{\partial V_{\text{KS}}}{\partial u_{\mu\kappa}(\mathbf{q})} - \frac{\partial \epsilon_i}{\partial u_{\mu\kappa}(\mathbf{q})} \right) |\psi_i\rangle. \quad (\text{A6})$$

Here  $H_{\text{KS}}$ ,  $V_{\text{KS}}$ , and  $\epsilon_i$  denote the Hamiltonian, self-consistent potential, and eigen energy of the Kohn-Sham system respectively. The derivative of the Kohn-Sham potential also depends on the electron density response:

$$\begin{aligned} \frac{\partial V_{\text{KS}}(\mathbf{r})}{\partial u_{\mu\kappa}(\mathbf{q})} &= \frac{\partial V_{ie}(\mathbf{r})}{\partial u_{\mu\kappa}(\mathbf{q})} \\ &+ \int \frac{1}{|\mathbf{r} - \mathbf{r}'|} \frac{\partial n(\mathbf{r}')}{\partial u_{\mu\kappa}(\mathbf{q})} d^3r' + \frac{dV_{xc}}{dn} \frac{\partial n(\mathbf{r})}{\partial u_{\mu\kappa}(\mathbf{q})} \end{aligned} \quad (\text{A7})$$

with the exchange-correlational potential  $V_{xc}$ . One can obtain the electronic density response, the Kohn-Sham wave function response, and the modulation of the potential simultaneously with solving Eqs. (A5 - A7) as a set of equations. These scheme is known as the Sternheimer method [48]. Also, the electron-phonon matrix element can be evaluated through this scheme since it also determined as follows:

$$\begin{aligned} g_{\lambda}^{i\mathbf{p}+\mathbf{q},j\mathbf{p}}(\mathbf{q}) &= \sum_{\kappa\mu} \sqrt{\frac{\hbar}{2M_{\kappa}\omega_{\mathbf{q}\lambda}}} \\ &\times \langle \psi_{i\mathbf{p}+\mathbf{q}} | \nabla_{l\kappa\mu} V_{\text{KS}} | \psi_{j\mathbf{p}} \rangle e_{\kappa}^{\mu}(\mathbf{q}\lambda), \end{aligned} \quad (\text{A8})$$

where  $\nabla_{l\kappa\mu}$  denotes the partial derivative with respect to the  $\kappa$ -th ion position in the  $l$ -th unit cell for the  $\mu$  direction. This is the formulation of density functional perturbation theory [48]. Here, one should notice that the calculated dynamical matrix and electron-phonon matrix element are statically renormalized quantities.

In practical calculation, in order to avoid the singular behavior in the l.h.s. of Eq. (A6), one introduces a projection operator. If Eq. (A6) is formally solved, the derivative of the wave function is written as

$$\left| \frac{\partial \psi_i}{\partial u_{\mu\kappa}(\mathbf{q})} \right\rangle = \sum_{j \neq i} \frac{\langle \psi_j | \partial V_{\text{KS}} / \partial u_{\mu\kappa}(\mathbf{q}) | \psi_i \rangle}{\epsilon_i - \epsilon_j} |\psi_j\rangle. \quad (\text{A9})$$

With this formulation, the electron density response is



given by

$$\frac{\partial n(\mathbf{r})}{\partial u_{\mu\kappa}(\mathbf{q})} = 4\text{Re} \sum_{i;\text{occ}} \sum_{j \neq i} \psi_i^*(\mathbf{r}) \psi_j(\mathbf{r}) \times \frac{\langle \psi_j | \partial V_{\text{KS}} / \partial u_{\mu\kappa}(\mathbf{q}) | \psi_i \rangle}{\epsilon_i - \epsilon_j}. \quad (\text{A10})$$

Eq. (A10) does not have a convenient form to solve directly because of the summation over the unoccupied states. However, due to the cancellation of the contribution involving occupied states, the summation over the index  $k$  in the r.h.s. of Eq. (A10) can be restricted to the unoccupied orbitals and the density response only depends on the change of the wave function in the unoccupied manifold. Therefore, one can evaluate the electron

density response with restriction of Eq. (A6) on the unoccupied manifold. It is achieved by following equation:

$$(H_{\text{KS}} + \alpha P_{\text{occ}} - \epsilon_i) \left| \frac{\partial \psi_i}{\partial u_{\mu\kappa}(\mathbf{q})} \right\rangle = -P_{\text{unocc}} \frac{\partial V_{\text{KS}}}{\partial u_{\mu\kappa}(\mathbf{q})} |\psi_i\rangle, \quad (\text{A11})$$

where  $P_{\text{occ}}$  and  $P_{\text{unocc}}$  are projection to the occupied and unoccupied spaces, and  $\alpha$  is a constant introduced in order to avoid the singularity of the operator  $H_{\text{KS}} - \epsilon_i$ . (For the selection of  $\alpha$  and more practical implementation, see e.g., Ref. [48].) One can show that the solution of Eq. (A11) is equivalent to that of Eq. (A6) on the unoccupied manifold.

- 
- [1] J. G. Bednorz and K. A. Müller Z. Phys. B **64**, 189 (1986).
  - [2] Y. Kamihara, T. Watanabe, M. Hirano, and H. Hosono, J. Am. Chem. Soc. **130**, 3296 (2008).
  - [3] N. W. Ashcroft, Phys. Rev. Lett. **21**, 1748 (1968).
  - [4] V. L. Ginzburg, J. Stat. Phys. **1**, 3 (1969).
  - [5] N. W. Ashcroft, Phys. Rev. Lett. **92**, 187002 (2004).
  - [6] J. Bardeen, L. N. Cooper, and J. R. Schrieffer, Phys. Rev. **108**, 1175 (1957).
  - [7] T. E. Weller, M. Ellerby, S. S. Saxena, R. P. Smith, and N. T. Skipper, Nat. Phys. **1**, 39 (2005).
  - [8] K. Shimizu, H. Ishikawa, D. Takao, T. Yagi, and K. Amaya, Nature (London) **419**, 597 (2002).
  - [9] V. V. Struzhkin, M. I. Erements, W. Gan, H. K. Mao, and R. J. Hemley, Science **298**, 1213 (2002).
  - [10] Theoretically, it has recently been shown that plasmons cooperate with phonons to enhance  $T_c$  in the lithium under pressure [R. Akashi and R. Arita, Phys. Rev. Lett. **111**, 057006 (2013)].
  - [11] J. Nagamatsu, N. Nakagawa, T. Muranaka, Y. Zenitani, and J. Akimitsu, Nature (London) **410**, 63 (2001).
  - [12] E. A. Ekimov, V. A. Sidorov, E. D. Bauer, N. N. Mel'nik, N. J. Curro, J. D. Thompson, and S. M. Stishov, Nature (London) **428**, 542 (2004).
  - [13] H. Okazaki, T. Wakita, T. Muro, T. Nakamura, Y. Muraoka, T. Yokoya, S. Kurihara, H. Kawarada, T. Oguchi, and Y. Takano, Appl. Phys. Lett. **106**, 052601 (2015).
  - [14] A. P. Drozdov, M. I. Erements, and I. A. Troyan, arXiv:1412.0406.
  - [15] A. P. Drozdov, M. I. Erements, I. A. Troyan, V. Ksenofontov, and S. I. Shylin, Nature (London) **525**, 73 (2015).
  - [16] C. W. Chu, L. Gao, F. Chen, Z. J. Huang, R. L. Meng, and Y. Y. Xue, Nature (London) **365**, 323 (1993).
  - [17] A. Schilling, M. Cantoni, J. D. Guo, and H. R. Ott, Nature (London) **363**, 56 (1993).
  - [18] Y. Li, J. Hao, H. Liu, Y. Li, and Y. Ma, J. Chem. Phys. **140**, 174712 (2014).
  - [19] D. Duan, Y. Liu, F. Tian, D. Li, X. Huang, Z. Zhao, H. Yu, B. Liu, W. Tian, and T. Cui, Sci. Rep. **4**, 6968 (2014).
  - [20] A. P. Durajski, R. Szczęśniak, and Y. Li, Physica C **515**, 1 (2015).
  - [21] J. E. Hirsch and F. Marsiglio, Physica C **511**, 45 (2015).
  - [22] N. Bernstein, C. S. Hellberg, M. D. Johannes, I. I. Mazin, and M. J. Mehl, Phys. Rev. B **91**, 060511 (2015).
  - [23] D. Duan, X. Huang, F. Tian, D. Li, H. Yu, Y. Liu, Y. Ma, B. Liu, and T. Cui, Phys. Rev. B **91**, 180502(R) (2015).
  - [24] D. A. Papaconstantopoulos, B. M. Klein, M. J. Mehl, and W. E. Pickett, Phys. Rev. B **91**, 184511 (2015).
  - [25] J. A. Flores-Livas, A. Sanna, and E. K. U. Gross, arXiv:1501.06336.
  - [26] R. Akashi, M. Kawamura, S. Tsuneyuki, Y. Nomura, and R. Arita, Phys. Rev. B **91**, 224513 (2015).
  - [27] I. Errea, M. Calandra, C. J. Pickard, J. Nelson, R. J. Needs, Y. Li, H. Liu, Y. Zhang, Y. Ma, and F. Mauri, Phys. Rev. Lett. **114**, 157004 (2015).
  - [28] A. Bianconi and T. Jarlborg, Europhys. Lett. **112**, 37001 (2015); Nov. Supercond. Mater. **1**, 37 (2015); T. Jarlborg and A. Bianconi, arXiv:1509.07451.
  - [29] Y. Li, L. Wang, H. Liu, Y. Zhang, J. Hao, C. J. Pickard, J. R. Nelson, R. J. Needs, W. Li, Y. Huang, I. Errea, M. Calandra, F. Mauri, and Y. Ma, arXiv:1508.03900.
  - [30] Y. Quan and W. E. Pickett, arXiv:1508.04491.
  - [31] C. Heil and L. Boeri, Phys. Rev. B **92**, 060508(R) (2015).
  - [32] Y. Ge, F. Zhang, and Y. Yao, arXiv:1507.0852.
  - [33] L. Ortenzi, E. Cappelluti, and L. Pietronero, arXiv:1511.04304.
  - [34] A. P. Durajski, R. Szczęśniak, and L. Pietronero, Ann. Phys. (Berlin), DOI:10.1002/andp.201500316 (2016).
  - [35] L. P. Gor'kov and V. Z. Kresin, arXiv:1511.06926.
  - [36] I. Errea, M. Calandra, C. J. Pickard, J. Nelson, R. J. Needs, Y. Li, H. Liu, Y. Zhang, Y. Ma, and F. Mauri, arXiv:1512.02933.
  - [37] R. Akashi, W. Sano, R. Arita, and S. Tsuneyuki, arXiv:1512.06680.
  - [38] M. Einaga, M. Sakata, T. Ishikawa, K. Shimizu, M. I. Erements, A. P. Drozdov, I. A. Troyan, N. Hirao, and Y. Ohishi, arXiv:1509.03156.
  - [39] A. B. Migdal, Zh. Eksp. Teor. Fiz. **34**, 1438 (1958) [Sov. Phys. JETP **7**, 996 (1958)].
  - [40] G. M. Eliashberg, Zh. Eksperim. i Teor. Fiz. **38** 966 (1960) [Sov. Phys. JETP **11** 696 (1960)].
  - [41] S. G. Lie and J. P. Carbotte, Solid State Commun. **26**,

- 511 (1978).
- [42] W. E. Pickett, Phys. Rev. B **26**, 1186 (1982).
- [43] W. E. Pickett, Phys. Rev. Lett. **48**, 1548 (1982).
- [44] B. Mitrović and J. P. Carbotte, Can. J. Phys. **61**, 758 (1983); Can. J. Phys. **61**, 784 (1983); Can. J. Phys. **61**, 872 (1983).
- [45] B. Mitrović and J. P. Carbotte, Phys. Rev. B **28**, 2477 (1983).
- [46] M. Lüders, M. A. L. Marques, N. N. Lathiotakis, A. Floris, G. Profeta, L. Fast, A. Continenza, S. Massidda, and E. K. U. Gross, Phys. Rev. B **72**, 024545 (2005); M. A. L. Marques, M. Lüders, N. N. Lathiotakis, G. Profeta, A. Floris, L. Fast, A. Continenza, E. K. U. Gross, and S. Massidda, Phys. Rev. B **72**, 024546 (2005).
- [47] It should be noted that the evaluation of the lowest order vertex correction is not a complete test to examine the validity of the ME theory.
- [48] S. Baroni, S. de Gironcoli, A. Dal Corso, and P. Giannozzi, Rev. Mod. Phys. **73**, 515 (2001).
- [49] It is a highly non-trivial problem whether we can avoid the double counting of two-particle interaction when we combine DFT and the Green's function theory.
- [50] M. S. Hybertsen and S. G. Louie, Phys. Rev. B **35**, 5585 (1987); Phys. Rev. B **35**, 5602 (1987).
- [51] D. Pines, "Elementary Excitations in Solids", Benjamin, New York, (1963).
- [52] Y. Takada, J. Phys. Soc. Jpn. **45**, 786 (1978).
- [53] D. Rainer, Prog. Low Temp. Phys. **10**, 371 (1986).
- [54] P. B. Allen and B. Mitrović, "Theory of Superconducting  $T_c$ ", Solid State Physics, **37**, 1 (1989).
- [55] F. Marsiglio and J. P. Carbotte, "Electron-Phonon Superconductivity" in Superconductivity, ed. by K. H. Bennemann and J. B. Ketterson, Springer, (2008).
- [56] P. Morel and P. W. Anderson, Phys. Rev. **125**, 1263 (1962).
- [57] F. Giustino, M. L. Cohen, and S. G. Louie, Phys. Rev. B **76**, 165108 (2007).
- [58] P. B. Allen and V. Heine, J. Phys. C **9**, 2305 (1976).
- [59] P. B. Allen and M. Cardona, Phys. Rev. B **24**, 7479 (1981); Phys. Rev. B **27**, 4760 (1983).
- [60] F. Giustino, S. G. Louie, and M. L. Cohen, Phys. Rev. Lett. **105**, 265501 (2010).
- [61] X. Gonze, P. Boulanger, and M. Côté, Ann. Phys. (Berlin) **523**, 168 (2011).
- [62] S. Poncé, G. Antonius, Y. Gillet, P. Boulanger, J. Laflamme Janssen, A. Marini, M. Côté, and X. Gonze, Phys. Rev. B **90**, 214304 (2014).
- [63] H. Y. Fan, Phys. Rev. **78**, 808 (1950); Phys. Rev. **82**, 900 (1951).
- [64] E. Antoncik, Czech. J. Phys. **5**, 4 (1955).
- [65] P. Poncé, G. Antonius, P. Boulanger, E. Cannuccia, A. Marini, M. Côté, and X. Gonze, Comp. Mater. Sci. **83**, 341 (2014).
- [66] Although the rigid-ion approximation is a good assumption for the DW term, it is known that this approximation sometimes fails to evaluate the electron-phonon coupling constant [D. Glötzl, D. Rainer, and H. R. Schober, Z. Physik B **35**, 317 (1979)].
- [67] G. Antonius, S. Poncé, P. Boulanger, M. Côté, and X. Gonze, Phys. Rev. Lett. **112**, 215501 (2014).
- [68] X. Gonze, B. Amadon, P. Anglade, J. Beuken, F. Bottin, P. Boulanger, F. Bruneval, D. Caliste, R. Caracas, M. Côté, T. Deutsch, L. Genovese, P. Ghosez, M. Giantomassi, S. Goedecker, D. Hamann, P. Hermet, F. Jollet, G. Jomard, S. Leroux, M. Mancini, S. Mazevet, M. Oliveira, G. Onida, Y. Pouillon, T. Rangel, G. Rignanese, D. Sangalli, R. Shaltaf, M. Torrent, M. Verstraete, G. Zerah, and J. Zwanziger, Comp. Phys. Comm. **180**, 2582 (2009); <http://www.abinit.org/>
- [69] P. Souvatzis, O. Eriksson, M. I. Katsnelson, and S. P. Rudin, Phys. Rev. Lett. **100**, 095901 (2008).
- [70] O. Hellman, I. A. Abrikosov, and S. I. Simak, Phys. Rev. B **84**, 180301 (2011).
- [71] I. Errea, M. Calandra, and F. Mauri, Phys. Rev. B **89**, 064302 (2014).
- [72] B. Monserrat, N. D. Drummond, and R. J. Needs, Phys. Rev. B **87**, 144302 (2013).
- [73] T. Tadano and S. Tsuneyuki, Phys. Rev. B **92**, 054301 (2015).
- [74] N. R. Werthamer, Phys. Rev. B **1** 572 (1970).
- [75] T. Tadano, Y. Gohda, and S. Tsuneyuki, J. Phys.: Condens. Matter **26**, 225402 (2014).
- [76] F. Zhou, W. Nielson, Y. Xia, and V. Ozoliņš, Phys. Rev. Lett. **113**, 185501 (2014).
- [77] P. Giannozzi, S. Baroni, N. Bonini, M. Calandra, R. Car, C. Cavazzoni, D. Ceresoli, G. L. Chiarotti, M. Cococcioni, I. Dabo, A. Dal Corso, S. Fabris, G. Fratesi, S. de Gironcoli, R. Gebauer, U. Gerstmann, C. Gougousis, A. Kokalj, M. Lazzeri, L. Martin-Samos, N. Marzari, F. Mauri, R. Mazzarello, S. Paolini, A. Pasquarello, L. Paulatto, C. Sbraccia, S. Scandolo, G. Sclauzero, A. P. Seitsonen, A. Smogunov, P. Umari, and R. M. Wentzcovitch, J. Phys.: Condens. Matter **21**, 395502 (2009); <http://www.quantum-espresso.org/>
- [78] J. P. Perdew, K. Burke, and M. Ernzerhof, Phys. Rev. Lett. **77**, 3865 (1996).
- [79] N. Troullier and J. L. Martins, Phys. Rev. B **43**, 1993 (1991).
- [80] O. Jepsen and O. K. Andersen, Solid State Commun. **9**, 1763 (1971).
- [81] M. Methfessel and A. T. Paxton, Phys. Rev. B **40**, 3616 (1989).
- [82] F. Giustino, J. R. Yates, I. Souza, M. L. Cohen, and G. Louie, Phys. Rev. Lett. **98**, 047005 (2007).
- [83] M. Kawamura, Y. Gohda, and S. Tsuneyuki, Phys. Rev. B **89**, 094515 (2014).
- [84] J. R. Schrieffer, "Theory of Superconductivity", Benjamin, New York, (1964).
- [85] For  $Im\bar{3}m$ -H<sub>3</sub>S ( $P\bar{1}$ -H<sub>2</sub>S),  $T_c$ 's are 217 K (54 K) with  $\omega_{el} = 10$  eV and 229 K (57 K) with  $\omega_{el} = 30$  eV.
- [86] Regarding the self-consistency, the DW term is independent of the electronic self-energy [61].
- [87] In the calculation of the ZPR, we use harmonic phonon frequencies. On the other hand, frequencies of bond-stretching phonons which have strong coupling with electrons are hardened due to the anharmonicity. Therefore, the effect of the ZPR might be mitigated by the anharmonicity.
- [88] In Ref. [27], it is reported that  $T_c$  decreases by 36 K (19 %) with anharmonic phonons in the H<sub>3</sub>S- $Im\bar{3}m$  structure at 250 GPa. This reduction is slightly larger than that in our calculation. Such difference can be attributed to the modulation of the phonon polarization vector, which is included in the calculation of Ref. [27] but ignored in ours.
- [89] In this study, we consider the same vertex correction both for the normal and anomalous part as in Ref. [92]. It is equivalent to assume for the vertex function to be proportional to  $\hat{\tau}_3$ , the  $z$ -component of the Pauli matrix.

On the other hand, the vertex correction can have contributions proportional to  $\hat{\tau}_1$  and  $\hat{\tau}_2$ , and enter in a different way in the normal and anomalous part [90]. It was suggested that these contributions are related with the interaction between electrons and collective modes in the superconducting state, which change into the plasmon modes [Y. Takada, J. Phys. Chem. Solids **54**, 1774 (1993); T. Gherghetta and Y. Nambu, Phys. Rev. B **49**, 740 (1994)].

[90] C. Grimaldi, L. Pietronero, and S. Strässler, Phys. Rev.

Lett. **75**, 1158 (1995); L. Pietronero, S. Strässler, and C. Grimaldi, Phys. Rev. B **52**, 10516 (1995); C. Grimaldi, L. Pietronero, and S. Strässler, Phys. Rev. B **52**, 10530 (1995).

[91] E. Cappelluti and L. Pietronero, Phys. Rev. B **53**, 932 (1996); Europhys. Lett. **36**, 619 (1996).

[92] Y. Takada, Phys. Rev. B **52**, 12708 (1995); Y. Takada and T. Higuchi, Phys. Rev. B **52**, 12720 (1995).